# Controlled Electrochemical Reduction of Gold and Palladium Metal Precursors in Polyaniline

Nicole Goodwin
*University of Nevada, Las Vegas*, nicolyngoodwin@gmail.com

CONTROLLED ELECTROCHEMICAL REDUCTION OF GOLD AND PALLADIUM

METAL PRECURSORS IN POLYANILINE


By


Nicole Goodwin


Bachelor of Science - Chemistry

University of Nevada, Las Vegas

2010


A dissertation submitted in partial fulfillment

of the requirements for the


Doctor of Philosophy – Chemistry


Department of Chemistry and Biochemistry

College of Sciences

The Graduate College


University of Nevada, Las Vegas

December 2017

UNLV | GRADUATE COLLEGE

**Dissertation Approval**

The Graduate College
The University of Nevada, Las Vegas

November 14, 2017

This dissertation prepared by

Nicole Goodwin

entitled

Controlled Electrochemical Reduction of Gold and Palladium Metal Precursors in Polyaniline

is approved in partial fulfillment of the requirements for the degree of

Doctor of Philosophy – Chemistry
Department of Chemistry and Biochemistry

David Hatchett, Ph.D.                                  Kathryn Hausbeck Korgan, Ph.D.
*Examination Committee Chair*                          *Graduate College Interim Dean*

Kathleen Robins, Ph.D.
*Examination Committee Member*

Spencer Steinberg, Ph.D.
*Examination Committee Member*

Shawn Gerstenberger, Ph.D.
*Graduate College Faculty Representative*

Abstract

Controlled Electrochemical Reduction of Gold and Palladium Metal Precursors in Polyaniline

By

Nicole Goodwin

Dr. David W. Hatchett, Examination Committee Chair
Professor of Chemistry
University of Nevada, Las Vegas

Polyaniline (PANI) has been extensively studied due to its unique electrochemical properties. The conjugated polymer is conductive with high chemical stability below 100°C, mechanical strength, and large surface area. The applications of PANI have included chemical sensing, corrosion inhibition coatings, light emitting diode and as a substrate for metal composite catalysts. Both chemical and electrochemical methods have been developed and utilized in the synthesis of PANI/metal composites. The simultaneous reduction of aniline and metal precursor produces a composite of PANI encapsulated metal, reducing the active surface area available for catalysis. Alternatively, chemical reduction of the metal precursor into preformed PANI produces deposits at the point of contact with the polymer but offers little control over the amount, dispersion, and size of the metal in the composite catalyst.

A method of electrochemically controlled uptake and reduction of Au and Pd metal precursors into PANI was developed. This method exploits the doping mechanism of polyaniline to distribute the metals throughout the polymer as it is oxidized. Deposition of the metal is achieved through the reduction of the polymer and the simultaneous reduction of the metal anion. The morphology of the composites was evaluated using SEM/EDX analysis. Electrochemically controlled metal oxide formation and reduction confirmed that the surface area of the metal in the

composite increased with each deposition scan. Both PANI/Au and PANI/Pd composites proved to be effective catalysts for propanol oxidation.

With an understanding of the deposition processes associated with single metal species, the synthesis of bimetallic PANI/AuPd composites was achieved. Previous work has shown that bimetallic catalysts often have higher catalytic efficiency and reduced poisoning when compared to their monometallic counterparts. Competition of the metals in the deposition process was evaluated by reducing Au and Pd simultaneously. In addition, the effect of deposition order was examined by depositing the metals sequentially. SEM/EDX analysis was used to examine the morphology and composition of all the composites. Metal oxide formation and reduction was used to probe the electrochemically distinct metal species within the polymer. Evidence of alloying was observed for most of the bimetallic composites. Propanol oxidation data showed that the bimetallic composites had higher catalytic efficiency when compared to PANI/Au and PANI/Pd.

Acknowledgements

Pursuing my Ph.D. has been the most difficult task I have ever encountered in my life, and I certainly could not have accomplished it on my own. I couldn't possibly hope to express the amount of gratitude I feel for the people who have pushed and inspired me in this seemingly endless pursuit, but I will try.

First, I would like to thank Dr. David Hatchett, my academic advisor. Without his guidance, wisdom, and patience (and barbecues), I would not be where I am today.

I would like to thank my committee members, Dr. Spencer Steinberg, Dr. Kathleen Robins, and Dr. Shawn Gerstenberger and for their endless support and encouragement.

I am eternally grateful to my family for their love and understanding. You were always there when I needed to vent and unwind. You provided that extra push I needed when I thought I wanted to quit. You have shaped me into the hard-working and strong young(ish) woman (I hope) I am today. And for that, I thank you.

To all my friends and fellow grad students who have supported me and shared my pain, thank you.

And finally, to all those who believed in me, even when I didn't believe in myself, thank you.

Table of Contents

# List of Tables

# List of Figures

Chapter 1 - Introduction

1.1 Polyaniline

Polyaniline (PANI) is a novel polymer that has been extensively studied because of its unique electronic properties. It is an intrinsically conductive polymer (ICP) with high mechanical strength, chemical stability, and a large three-dimensional surface area. The conductivity of the polymer can be varied by changing the oxidation state and through acid doping. These properties have been exploited to produce chemical sensors[1,2,3], corrosion inhibition coatings[4,5], light emitting diodes[6,7], and low-cost microelectronics[8].

1.1.1 Intrinsically Conductive Polymers

In the year 2000 Alan J. Heeger, Alan G. MacDiarmid, and Hideki Shirakawa were awarded the Nobel Prize in chemistry for their discovery and development of intrinsically conductive polymers (ICPs). Prior to their work, polymers were considered to be insulating plastics; the perfect material to protect against heat and electricity. However, they found that some polymers, including polyacetylene, polypyrrole, and PANI exhibited almost metallic conductivity when they were doped with an acid, halide, or alkali metals.

In his Nobel Prize lecture[9], Heeger enumerates three advantages of using ICPs over metals or inorganic semiconductors in some applications. First, there are several possible methods of synthesizing ICPs because of their solubility in common solvents. Two such methods include 1) spin-casting polymers from solution into a thin film, and 2) inducing polymerization using a molecular template as a substrate. Second, ICPs can be synthesized to be transparent over a desired range of wavelengths. Transparency is imperative for applications such as photodiodes (photon induced generation of electricity) and light emitting diodes (electricity induced generation of photons). Lastly, the Fermi energy can be controlled. A device using an ICP as an electrode can

be designed to achieve a desired band gap that can absorb (photodiodes) or emit (LEDs) desired wavelengths of light.

The first ICP to be examined was polyacetylene (PA). Shirakawa, et al[10], exposed PA films to bromine for several minutes, which resulted in the following reaction with the polymer:

$$[CH]_n \ + \ \left(\frac{nx}{2}\right) Br_2 \ \rightleftharpoons \ [CHBr_x]_n$$
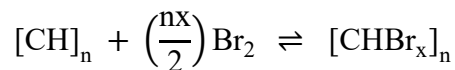
PA films were also exposed to iodine vapors, resulting in doping of the polymer according to the following reaction:

$$[CH]_n \ + \ \left(\frac{nx}{2}\right) I_2 \ \rightleftharpoons \ [CHI_x]_n$$
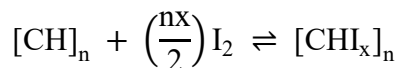
The conductivity of the PA films increased from 3.2 x $10^{-6}$ S/cm to 0.5 S/cm and 38 S/cm after doping with bromine and iodine, respectively. In addition, it was determined that the conductivity changed as a function of exposure time. Therefore, the conductivity of PA could be controlled by changing the dopant molecule or by varying the amount of dopant in the polymer structure. The conductivities of a selection of ICPs are summarized in **Table 1** with a variety of dopants. For comparison, the conductivities of ICPs prior to doping range from $10^{-10}$ to $10^{-5}$ S/cm.[11] This discovery of the tunable conductivity of ICPs initiated a new field of polymer chemistry research that captivated the scientific minds of various disciplines for decades.

**Table 1.** Conductivities of common conductive polymers.

| ICP | Doped Conductivity (S/cm) | Dopant | Reference |
|---|---|---|---|
| Trans-polyacetylene | 0.5 | $Br_2$ vapor | [10] |
| Trans-polyacetylene | 38 | $I_2$ vapor | [10] |
| Polyaniline | 5 | HCl | [12] |
| Poly(*p*-phenylene vinylene) | 3 | $AsF_5$ | [13] |
| Polypyrrole | 10-65 | $LiClO_4$ | [14] |

Some common ICPs and their structures are presented in **Figure 1**. Most of the polymers have highly-conjugated, electron-rich polymer backbones (e.g. PA) with the rest conjugated through doping (e.g. PANI). Doping the polymer generates delocalized charge carriers (i.e. electrons or holes) that can travel along the π-conjugated backbone. Doping is primarily achieved through oxidation or reduction of the polymer through chemical or electrochemical means, or via photoexcitation, where the uptake of ionic species balances charge.[9,15]
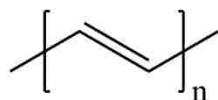
Polyacetylene
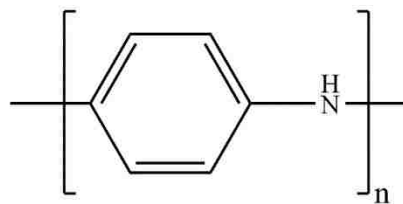
Polyaniline
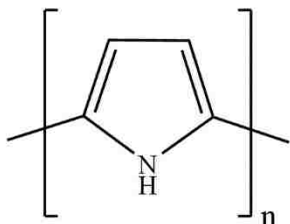
Polypyrrole
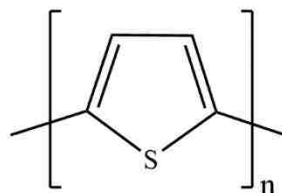
Polythiophene
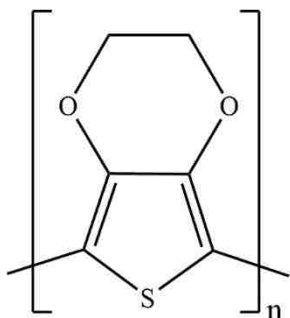
Poly(3,4-ethylene-dioxythiophene), PEDOT
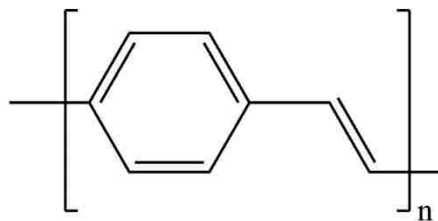
Poly(phenyl vinylene), PPV

**Figure 1.** Common intrinsically conducting polymers, undoped.[16]

For example, the redox doping of *trans*-PA with iodine is summarized by the following reaction:

$$[CH]_n + \left(\frac{3x}{2}\right)I_2 \rightleftharpoons [CH]_n^{x+} + xI_3^-$$
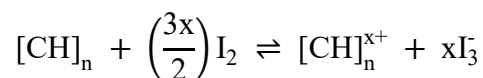
The iodine molecule oxidizes the polymer, removing an electron from the valence band of the polymer, creating a positively charged "hole." The negatively charged triiodide molecule is formed in the process.[17] Conduction is facilitated when a potential is applied, causing an electron from a neighboring atom to "jump" to the ionized atom to fill the hole. The continued transfer of

electrons gives the appearance of a hole traveling down the polymer. This is an example of p-type doping because a positively-charged charge carrier is generated. The triiodide molecule remains electrostatically bound to the polymer, stabilizing the polymer and neutralizing the positive charge, so the polymer remains neutral overall. Alternatively, *trans*-PA can undergo n-type doping with a reducing agent, such as sodium naphthalide.

$$[CH]_n + xNa^+C_{10}H_8^- \rightleftharpoons [CH]_n^{x-} + xNa^+ + xC_{10}H_8$$
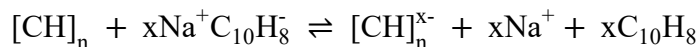
The dopant reduces the polymer, injecting an electron into its conduction band. When a potential is applied, the electron flows along the polymer backbone, through the conduction band. The sodium counterion stabilizes the negatively charged polymer. While both p-type and n-type doping are possible, p-type tends to be the preferred method because it produces more stable charge carriers.[18]

### 1.1.2 PANI Conductivity

PANI is an intrinsically conducting polymer that, when doped with acid, allows charge transfer through the conjugated polymer backbone. PANI is unique among conductive polymers because it can be both proton and anion doped, which can be utilized to vary and change both the chemical and electronic properties of the polymer. While most ICPs must undergo oxidation or reduction to achieve their conductive state, PANI is doped via an acid-base reaction that results in no net change in electrons along its conjugated backbone.[8,9] To understand PANI's unique conductivity, one must first examine its structure.
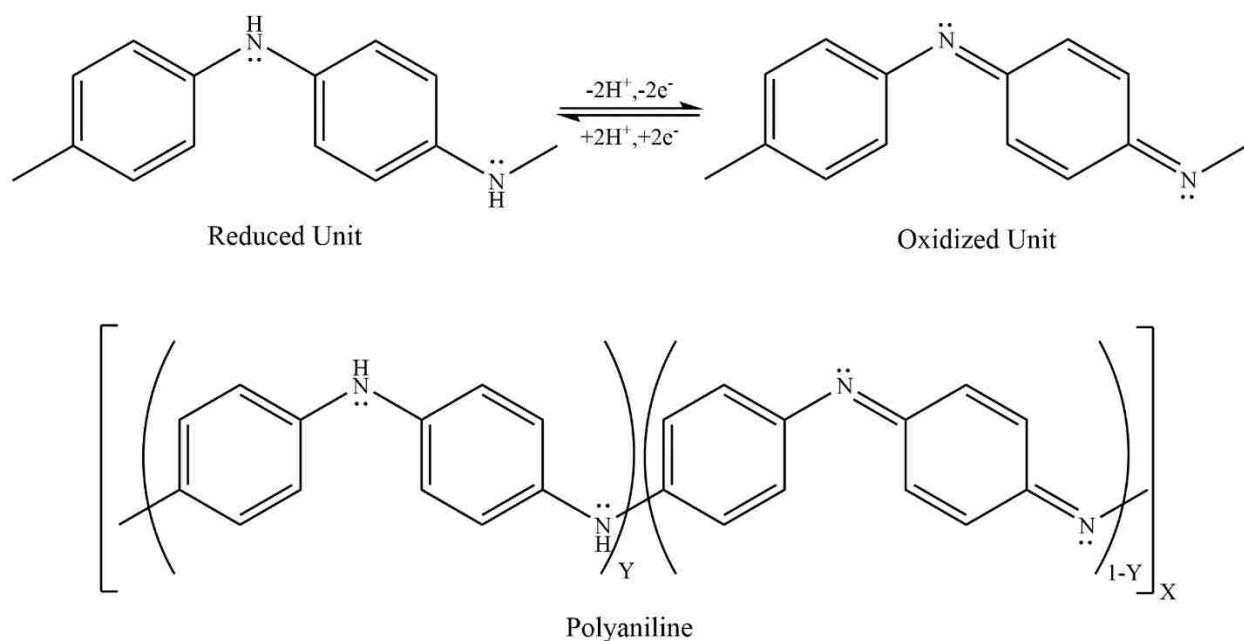
**Figure 2.** Structure of polyaniline.[8]

PANI is comprised of a combination of 2 distinct units: 1) reduced units of two benzenoid rings and two amine nitrogen atoms, and 2) oxidized units containing a benzenoid ring, a quinoid ring, and 2 imine nitrogen atoms, **Figure 2**. The oxidation state of the polymer is determined by the ratio of oxidized units to reduced units. The common oxidation states presented in **Figure 3** are the reduced form leucoemeraldine (Y = 1), the oxidized form pernigraniline (Y = 0), and emeraldine base (Y = 0.5) which contains an equal number of oxidized and reduced units. Doping of the emeraldine base with acid results in the $\pi$-conjugated emeraldine salt form, which is the most conductive form of PANI.
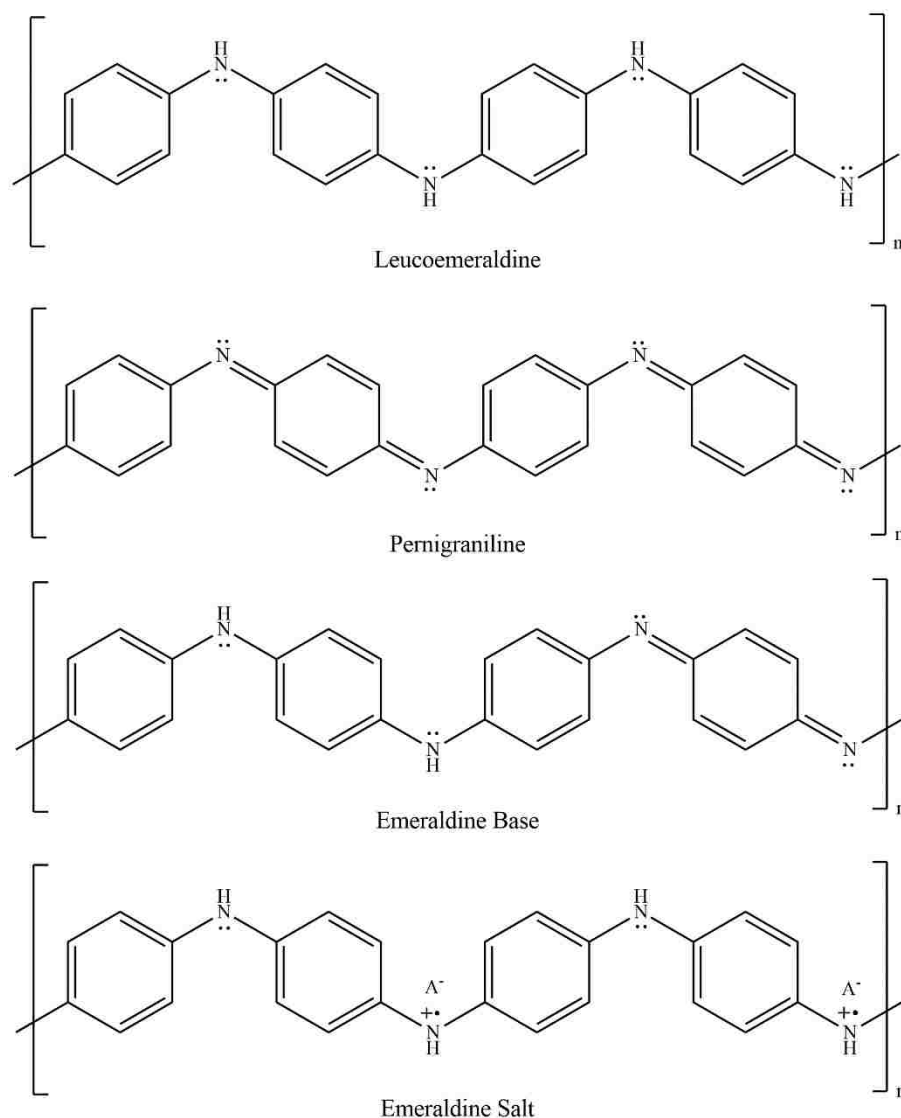
**Figure 3.** Oxidation states of PANI.[8]

The conductivity of PANI is best described using the polaron model, as seen in **Figure 4**. First, the imine nitrogen atoms ($pK_a$=5.5)[19] are protonated by the acid dopant. To stabilize the positively charged nitrogen atoms the polymer undergoes an internal redox reaction, reducing the quinoid ring to a benzenoid ring. As a result, the positively charged nitrogen atoms are oxidized, leaving a hole at each nitrogen in the valence band. The positively charged hole is called a polaron. Finally, there a redistribution of charge to separate the polarons and stabilize the molecule.[20]

Overall, the number of electrons along the polymer backbone remains the same, however the redistribution of charge due to the acid doping increases conjugation and creates two charge carriers per tetrameric unit, facilitating conductivity. However, just as with oxidative and reductive doping, the dopant anion remains coulombically bound to the polymer to maintain charge neutrality. Therefore, the redox state, the level of doping, and the identity of the dopant are important in the targeted electronic properties of the material[21]. Also, aniline conductivity is limited to applications in acidic media because of the acid-doping requirement. However, as will be discussed in Section 1.2, PANI "doped" by metals will retain its conductivity in alkaline environments.
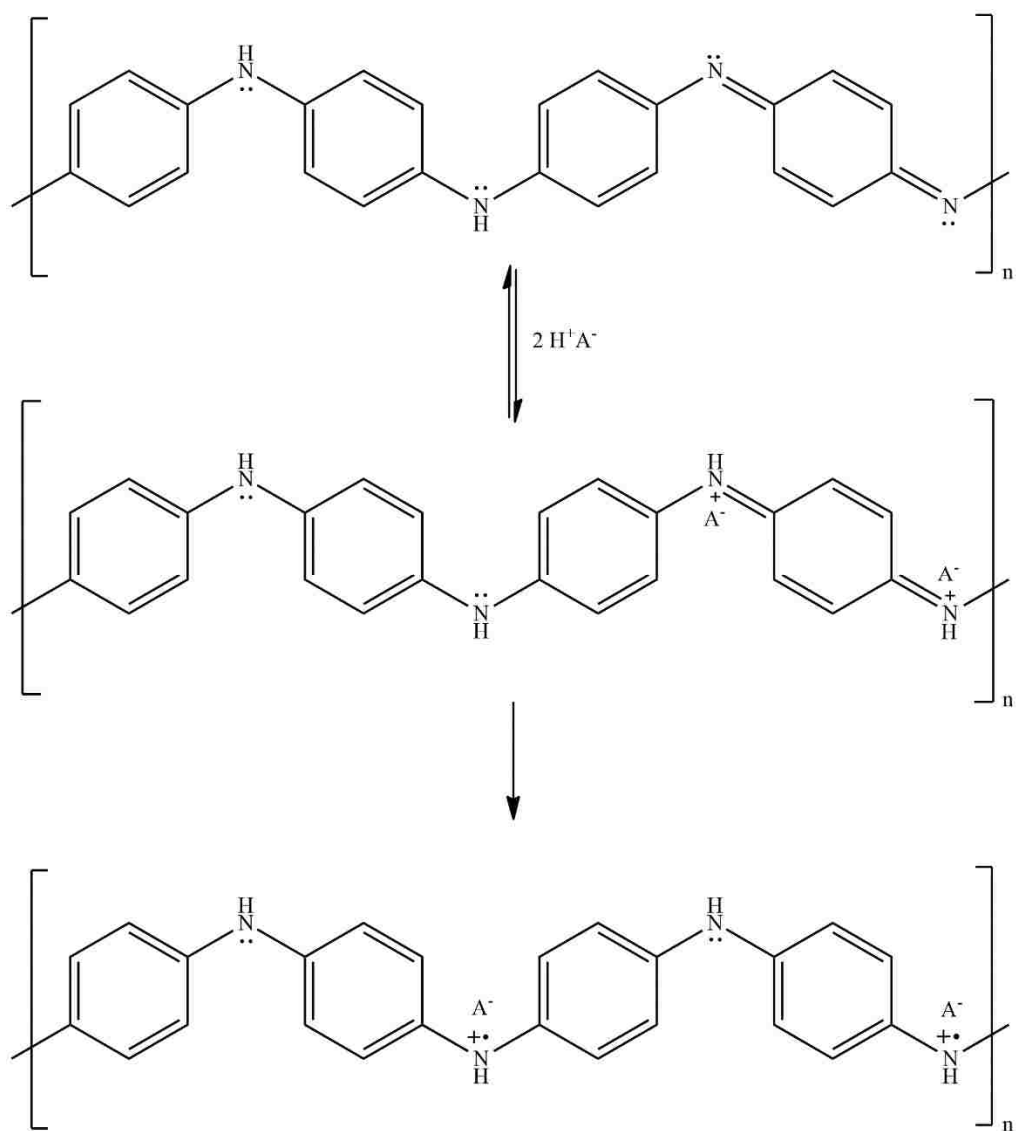
**Figure 4.** Polaron model of PANI conductivity.[9]

In addition, band structure is an important factor in determining the conductivity of a material. Differences in band structure can be accompanied by color changes of the material, because the band gap of a material determines what wavelengths of light it absorbs. Each oxidation state of PANI produces a different color; leucoemeraldine is yellow or colorless, emeraldine base is blue, and pernigraniline is violet or black. The green emeraldine salt form must have the ideal band structure to allow for charge transport. The changes in color confirm different band

structures, which could explain why emeraldine salt is conductive while leucoemeraldine and pernigraniline are not.

### 1.1.3 PANI Synthesis

Since the first experiments with the polymerization of aniline were reported by Runge in 1834, interest in the novel "black/dark green/dark blue/dark violet" product known as aniline black has grown. He found that heating a mixture of aniline nitrate and copper (II) chloride produced a product with a dark green color. In the early 1840s, Fritzsche oxidized an aniline salt using chromic acid, which produced a precipitate that turned from dark green to bluish-black. Electrochemical polymerization, reported by Letheby in 1862, resulted in a dark blue product.[20] In the 180 years since Runge's experiments, both chemical and electrochemical methods have been thoroughly investigated with varied results. Generally, they combine aniline with an oxidant (a chemical or an electrode) in an acidic solution. However, both methods have their own advantages and disadvantages.

The chemical synthesis of polyaniline has evolved drastically since Runge's experiments. In their 1990 review of PANI, Geniès, et al. summarize the various conditions that have been used to synthesize PANI. Their list of oxidants includes potassium dichromate, ammonium persulfate, hydrogen peroxide, ceric nitrate, and ceric sulfate.[22] Ciric-Marjanovic's 2013 review expanded this list to include other transition metal and noble metal compounds, including Mn(III), Mn(IV), Mn(VII), V(V), Cu(II), Au(III), Pt(IV), Pd(II), and Ag(I) compounds, although ammonium persulfate is the most common oxidant.[20] In addition, a pH of < 2 is typically maintained using HCl, $H_2SO_4$, or other strong acids. Oxidation of the aniline molecule results in the formation of a radical cation. Cations can react in a number of ways to produce a variety of different products depending on the reaction conditions including, oxidant strength, pH, aniline concentration, and

aniline/oxidant ratio. The aniline molecules form a radical cation that bond primarily in the para position due to steric interaction. There are three configurations that can result from this bonding: "head-to-head" bonding resulting in azobenzene or hydrazobenzene, "tail-to-tail" bonding forming benzidine, or "head-to-tail" bonding forming 4-aminodiphenylamine or *N*-phenyl-1,4-benzoquinonediimine, the precursors of polyaniline. The two former reactions form oligomers that can be found in the solution or trapped in the polymer. However, the "head-to-tail" bonding results in long PANI strands that precipitate out of solution.[20]

Electrochemical synthesis of PANI was first reported by MacDiarmid, et al.[23] A platinum foil electrode was immersed in a solution of aniline and HCl. The potential was cycled between -0.2 V and +0.75 V vs. SCE, causing polyaniline to "grow" onto the electrode surface. **Figure 5** presents the proposed mechanism for the electropolymerization of aniline. The electrochemical synthesis is initiated in similar manner when compared to chemical synthesis of PANI. Specifically, the potential dependent oxidation of aniline monomers forms the same aniline radical cation. The aniline monomers then continue to bond in a "head-to-tail" fashion, forming longer chains. After ~45 cycles, a film with a thickness of ~0.2 μm was produced at the electrode surface. The authors of this study do not explain in detail how the thickness was measured and correlated with the charge associated proton expulsion in the polymer. Therefore, we use this value only as an estimate of thickness and as an evaluation method for polymer synthesis reproducibility.

**Figure 5.** Electrochemical polymerization of aniline.[8]

Electrochemical doping was used to further characterize the electrochemically synthesized polymer. They found the electrode potential determined the oxidation state of the polymer when the electrode was immersed in an HCl solution and the potential was cycled from -0.2 V to 1.0 V vs. SCE. The data is presented by **Figure 6** and summarized in **Table 2**. As the potential is swept from 0.5 V to 1.0 V, the PANI film became violet, corresponding to the oxidation of PANI to the pernigraniline form. Peak A is the response to the migration of anion species to neutralize the newly oxidized film. Conversely, as the scan was reversed, the anion species were expelled (peak A') in response to the reduction of the polymer to the emeraldine form. As the anodic scan continued, the color of the film changes from blue to light green depending on whether there were more oxidized units (Y < 0.5) or more reduced units (Y > 0.5). Finally, peak B corresponds to the

migration of $H^+$ atoms in response to the reduction of the film to the yellow leucoemeraldine form, while peak B' is the result of the reverse process.

**Table 2.** Color of PANI oxidation states when acid doped.

| Potential (vs. Ag/AgCl) | Oxidation State | Color |
|---|---|---|
| E > 0.75 V | Pernigraniline | Violet |
| 0.75 V > E > 0.10 V | Emeraldine | Green |
| E < 0.10 V | Leucoemeraldine | Yellow |
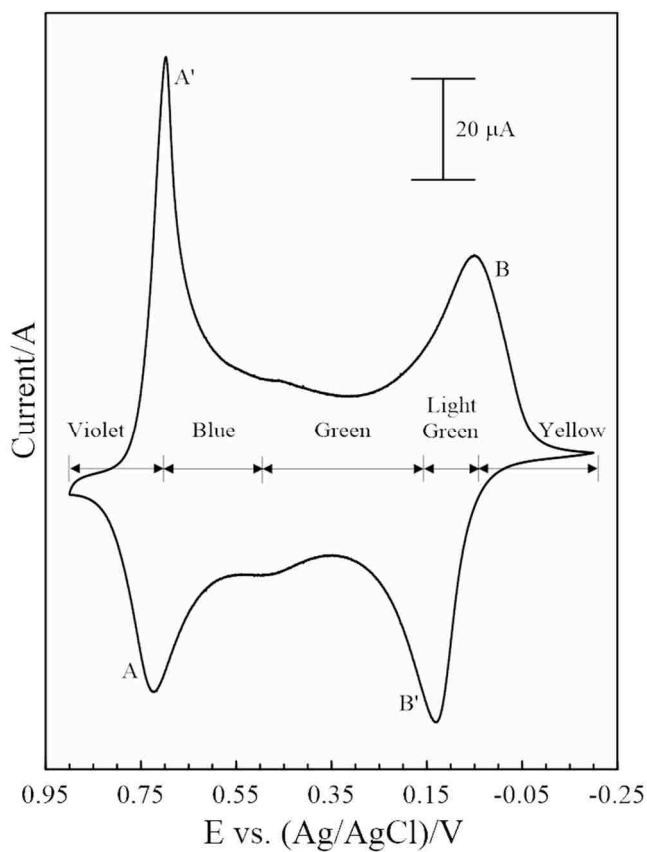


**Figure 6.** Electrochemical acid doping of PANI as described by MacDiarmid et al.[23]

The electrochemical polymerization of aniline has been investigated thoroughly over the past 30 years. Cyclic voltammetry continues to be an efficient method of PANI synthesis, however galvanostatic (constant current) and potentiostatic (constant potential) methods are utilized as well. A wide range of electrodes have been employed, from more conventional inert electrodes like Pt and conducting glass, to metals such as Au, Fe, and Cu, and conductive nonmetals such as glassy carbon, graphite, and n-type Si.[8] The primary advantage of electrochemical polymerization of aniline is control. The thickness and oxidation state of the film is more easily controlled when synthesized electrochemically than chemically. The product is also much cleaner since it does not require additional chemicals to initiate oxidation. However, the one advantage of chemical synthesis over electrochemical synthesis is the ability to produce PANI in much larger quantities.

1.2 PANI/metal Composites

The high surface area and electronic properties of PANI make it an effective material for developing polymer/metal catalytic membranes. PANI/metal composites such as PANI/Pt[24,25,26], PANI/Au[27,28,29], and PANI/Pd[30,31,32], have been extensively studied as catalytic membranes for alcohol oxidation reactions in both acidic and alkaline solutions. These studies have shown that there are advantages to the deposition of noble metals in PANI. The three-dimensional structure of PANI provides a template for developing relatively large catalytic surface areas in comparison to bulk two-dimensional metal catalyst surfaces. PANI has also been shown to exhibit a promoting effect by influencing the electronic properties of the catalyst resulting in enhanced catalytic activity and decreased poisoning.[33,34]

The uptake and dispersion of precursor metals species including $AuCl_4^-$, $PdCl_4^{2-}$, and $PtCl_4^{2-}$ into PANI is achieved using the normal anion doping of the polymer. Moreover, inclusion of ~20 % metal content of each metal species eliminates the need to acid dope PANI to maintain

the conductivity.  Therefore, the useful pH range of PANI based materials can be extended into alkaline environments that have been traditionally precluded.  The benefit of working at high pH is that surface poisoning can be reduced when alcohol oxidation takes place in the presence of hydroxide.[35,36]

### 1.2.1 PANI/metal Composite Synthesis

PANI/metal composites can be synthesized either chemically or electrochemically with variable results.  In chemical synthesis, aniline monomer is combined with either the pre-reduced metal or a metal precursor that can be reduced in a solution.  Then an oxidant such as ammonium persulfate is combined with the solution to initiate polymerization.  The emergent polymer can nucleate on the pre-formed metal to form the composite. Similarly, the metal precursor is reduced by the emerging polymer in-situ to produce the PANI/metal composite. In both cases the metal species is trapped in the emergent polymer during the synthesis, which minimizes the metal surface area available for catalysis.  Alternatively, preformed PANI can be mixed with a metal precursor in the presence of a reducing agent like $NaBH_4$.  In this case the metal deposits on the existing PANI and is not extensively encapsulated.  However, the method provides very little control over the particle size, dispersion, or the overall metal surface area.  Moreover, the oxidation state of the polymer is altered through the reduction of the metal species.  Although chemical synthesis can be utilized to produce bulk quantities of PANI/metal composites the process produces inhomogeneous composites that often contain trapped oligomers with other chemical species.

Electrochemical methods can be utilized to control the uptake, dispersion, and reduction of metal precursors in PANI.  Electrochemical methods allow the metal composition to be precisely controlled and varied producing composites with variable composition and morphology in comparison to composites produced chemically.  Electrochemically prepared PANI membranes

are produced in solutions containing the aniline monomer and acid electrolyte to ensure the PANI remains conductive.  The uptake and dispersion of metal anion precursors, $AuCl_4^-$ for example, can be achieved using the normal anion doping as the polymer is oxidized.  As PANI is oxidized the uptake of anion metal precursor occurs to maintain charge neutrality in the polymer.  The metal anion is dispersed based on the electrostatic charge in the polymer.  When PANI is then reduced, the metal anion is reduced into the polymer and chloride ions are expelled.    This process can be repeated to achieve PANI/metal composites with variable metal content.  While electrochemical synthesis allows for significantly more control over the PANI thickness and metal composition over chemical methods, it suffers in its inability to produce composites on a large, commercial scale.

### 1.2.2 Bimetallic Composites

Single metal PANI/metal composites are prone to surface poisoning at elevated pH through the formation of metal oxides and surface adsorption of oxidative products. Therefore, despite the enhanced electronic properties, there are limitations associated with using single metal composites for alcohol oxidation.  In contrast, bimetallic catalysts have been evaluated in an effort to reduce surface poisoning and increase catalytic activity relative to single metal systems.[37,38,39,40] The mechanism for the reduced poisoning at bimetallic catalysts is still open for debate; however, two possible explanations are that it is related to the electronic effect and the bifunctional effect.

The electronic effect involves interactions between two metal species that cause a shift in the electronic properties of the catalyst's surface, reducing surface interactions with poisoning species.  An example of this effect is observed in the oxidation of formic acid using a Au/Pd core-shell nanoparticle catalyst.  According to XPS studies the Pd shell had a lower binding energy than pure Pd black.  As a result, it was found that oxidation at the core-shell nanoparticles occurred

over a larger potential window than at Pd black because they were less prone to poisoning by OH⁻ and CO.[41]  Alternatively, the bifunctional effect results from each metal's affinity for different functional groups.  Different metals adhere to different functional groups in the molecule allowing for a more stable transition state and thus more efficient catalysis.  One study investigated the oxidation of alcohols and polyols over Au-Pd bimetallic catalysts.  The results suggested that the transition state of the molecule to be oxidized was stabilized through simultaneous interaction with the Pd species through an alkyl hydrogen and the Au species through the deprotonated oxygen.[42]  In addition, studies have shown examples where solvent molecules adsorb onto one metal species preferentially, which can then react with poisoning species on the other metal species to form chemical species that are easier to remove from the catalyst surface.  One example examines Pt-Ru bimetallic catalysts for the oxidation of methanol.  It was proposed that the Ru species became hydrated while methanol adsorption occurred at Pt.  The water became deprotonated, forming RuOH with the desorbed OH⁻ reacting with adsorbed poisoning species, cleaning the surface of contaminants.[43]  Similarly, another study showed Sn and Pb could be used as "oxygen-adsorbing" species to clean the Pt surface during the catalytic oxidation of ethylene glycol.[44]  It is possible that a combination of both the electronic and bifunctional effects results in reduced poisoning and increased efficiency.

1.3 Research Hypothesis

PANI/bimetallic composites have been studied in diverse application using a variety of metal combinations.  PANI/Ag-Mn has been investigated as a possible chemical sensor of *E. coli*.[45] PANI/La-Cd catalyzes photodegradation of organic pollutants.[46] The antimicrobial properties of PANI/Pt-Ag[47] and PANI/Pd-Au[48] have been studied for medical applications such as wound dressings, medical device coatings and "smart clothing."  By far the most widely researched

application of PANI/bimetallic composites is catalysis, especially for the oxidation of small organic molecules for use in fuel cells.[37,49,50,51,52,53] However, the methods utilized for synthesizing PANI/bimetallic composites have produced materials with variable results in terms of catalytic efficiency.

This dissertation probes the hypothesis that the controlled uptake and reduction of metal anion precursors is critical in defining both the physical and electronic properties of PANI composites. Moreover, the controlled reduction and deposition of metal species in PANI can result in alloying of metals to produce novel physical and chemical properties that are distinct in comparison to the individual species. The hypothesis is explored through the deposition of a single metal species to form PANI/Pd and PANI/Au composites using linear sweep voltammetry. The studies establish the parameters for the controlled uptake, dispersion, and reduction of individual metal species. With a thorough understanding of these processes the synthesis of PANI/Au-Pd bimetallic composites is evaluated using both the simultaneous and sequential deposition of the metals. Simultaneous deposition evaluates how competitive processes influence the overall electronic properties of the materials and any possible alloying of the species within PANI. Similarly, sequential deposition of Au and Pd evaluates the influence of existing metal deposits on the subsequent deposition of a second metal species and metal alloying in PANI. Finally, the results are summarized and the use of controlled electrochemical reduction of metal species in the formation of PANI/bimetallic composites with novel physical and chemical properties is discussed relative to the overall hypothesis.

Chapter 2 - Experimental Methods

2.1 Chemicals

Perchloric acid, $HClO_4$ (J.T. Baker, 69-72%, 9652-33), potassium hydroxide, KOH (Alfa Aesar, 99.99%, AA44273-36), n-propanol, $CH_3CH_2CH_2OH$ (Alfa Aesar, 99%, A19902), potassium tetrachloropalladate, $K_2PdCl_4$ (Strem, 99%, 10025-98-6), and potassium tetrachloroaurate, $KAuCl_4$ (Aldrich, 98%, 334545) were used as received. Aniline, $C_6H_5NH_2$ (Aldrich, 99.9%, 13,293-4) was distilled prior to use. All solutions were prepared using 18.3 MΩ•cm water obtained from a Barnstead E-pure water filtration system.

2.2 Electrochemical Synthesis of PANI/metal Composites

Electrochemical measurements were performed in a three-electrode cell using a CH Instruments 660E potentiostat with included software. A Pt sheet was used as the counter electrode with an immersed area that exceeded the working electrode by a factor of two. All potentials are referenced to the Ag/AgCl electrode (3 M KCl filling solution). An Au disc electrode was used as the working electrode for the electrochemical experiments (A = 0.02 cm$^2$). Au-plated mica was used as the working electrode for the SEM and EDX samples. All solutions were purged with nitrogen gas for 10 minutes before they were used in electrochemical experiments.

Polyaniline was electrochemically grown onto the working electrode from a solution of 0.250 M aniline and 1 M $HClO_4$ and cycling the potential between -0.2 V and +0.9 V for 10 complete voltammetric cycles at a scan rate of 10 mV/s. As described in the introduction, the aniline must be polymerized from an acidic solution with a pH below 4 to sufficiently grow films and to maintain conductivity through acid doping. There are multiple reasons why $HClO_4$ was used as the acid electrolyte for the polymerization of aniline. Traditionally $H_2SO_4$ and HCl are used, however, the polymer begins to degrade at oxidizing potentials when in the presence of these

acids.[54,55] Additionally, polyaniline films polymerized from $HClO_4$ have a smoother morphology when compared to those from $H_2SO_4$.[56] The resulting PANI-modified electrodes were thoroughly washed with ultrapure water.

For single metal studies, metal deposition was initiated using linear scan voltammetry (LSV) by immersing the PANI electrode into one of the following solutions containing metal precursors: 5 mM $KAuCl_4$ (PANI/Au) or 5 mM $K_2PdCl_4$ (PANI/Pd). The metal precursor solutions had pH values of 2.88 and 3.85 respectively, so the addition of acid electrolyte was not necessary to maintain PANI conductivity. In fact, the addition of acid electrolyte to the metal precursor solutions was avoided to prevent competing reactions with PANI that would prevent the reduction of the metal precursor in the polymer. The electrode was held at +1 V for two minutes to ensure metal anion was allowed to migrate to all possible oxidized sites in PANI so maximum metal deposition could be achieved. The electrode was poised at +1 V prior to immersion to prevent spontaneous reduction of metal into PANI. Metal was reduced by a cathodic scan to a final potential of -0.2 V at a scan rate of 10 mV/s. The reduction of the metal precursors results in the liberation of $Cl^-$ into the polymer and solutions. The resulting PANI/metal composite electrode was promptly removed from metal precursor solution and washed with copious amounts of ultrapure water. The process was repeated for a total of five scans. Electrochemical characterization of the composite was examined after each deposition scan.

Bimetallic composites were deposited into PANI films using the same electrochemical parameters described above, however, they were deposited either simultaneously from a single metal precursor or sequentially by alternating deposition with single metal precursor solutions. Simultaneous deposition of metals was achieved by performing five deposition scans using one of the following metal precursor solutions: 2.5 mM $KAuCl_4$ and 2.5 mM $K_2PdCl_4$ (PANI/1Au1Pd),

3.33 mM KAuCl$_4$ and 1.67 mM K$_2$PdCl$_4$ (PANI/2Au1Pd), or 1.67 mM KAuCl$_4$ and 3.33 mM K$_2$PdCl$_4$ (PANI/1Au2Pd).  Metals were deposited sequentially by first depositing five scans of Au or Pd, followed by deposition of Pd or Au for 1-5 scans.  Composites with Au deposited first are labeled PANI/5Au/xPd, where x denotes the number of deposition scans of Pd used for synthesis.  Alternatively, PANI/5Pd/xAu signifies that Pd was deposited first, followed by x cycles of Au.

2.3 Characterization

PANI/metal composites were characterized using three methods: acid doping, scanning electron microscopy (SEM), and energy dispersive spectroscopy (EDS).  Acid doping not only ensures that the PANI electrode is conductive, but also determines the approximate thickness of the PANI films.  SEM provides insight into the morphology of the composites.  Finally, EDS is used to confirm the metals have been incorporated into the composites.

2.3.1 Acid Doping

Acid doping was performed to ensure all PANI membranes had a consistent thickness.  The PANI electrodes were immersed in a solution of 1 M HClO$_4$ and held at a potential of +0.9 V for 2 minutes to condition the electrode.[57]  The potential was then cycled from +0.9 V to -0.2 V at 10 mV/s until steady state was achieved.  The average PANI thickness was estimated based on the average charge density for the proton expulsion for three PANI electrodes ($19150 \pm 2516$ µC/cm$^2$).  An estimated thickness of $240 \pm 31$ µm was obtained using the relationship that 80 µC/cm$^2$ corresponds to a 1 µm thickness.[58]  The standard deviation is based on the average of 3 electrodes.

2.3.2 Scanning Electron Microscopy (SEM) and Energy Dispersive Spectroscopy (EDS)

SEM images were acquired using a JEOL JSM 6700F Field Emission SEM instrument.  Surface pretreatment of the samples was not required because they are already conductive.  An accelerating voltage of 8.0 kV was used to image pristine PANI and all PANI/metal composites.

All images were obtained using a backscatter electron detector to provide a better contrast between metal and polymer than a secondary electron detector would provide. EDS spectra were obtained using a JEOL JSM 5610 scanning electron microscope equipped with an Oxford Instruments ISIS EDS system. An accelerating voltage of 8.0 kV was used to ensure the electron beam only measured the PANI composites and not the Au mica substrate.

2.4 Electrochemistry of PANI/metal composites in alkaline solution

Electrochemical studies for metal oxide formation/reduction and oxidation of propanol were performed to probe the electronic properties of the PANI/metal composites. The results of the PANI/Pd and PANI/Au studies were compared to bimetallic studies to determine if the metals react within the composite to create novel catalysts or if they work independently of each other.

2.4.1 Oxide formation and reduction at PANI/metal surface

Examining the electrochemical response of PANI/metal composites in alkaline solution provides important information regarding the chemical and physical properties of the material. First, the PANI/metal composites are studied in environments that preclude proton doping to determine if they maintain their conductivity in high pH environments. The conductivity is directly related to changes in the physical properties after metal inclusion. In addition, the formation and reduction of metal oxide is used to probe the reactivity and estimate the electrochemically active surface area of the metal deposited in the polymer.[59] Finally, electrochemical analysis of the composites can yield information regarding the formation of bimetallic composites and provide insights into how the metals interact with each other. Specifically, Au oxides and Pd oxides are formed and reduced at very distinct potentials that may be different when they are combined to form bimetallic deposits in PANI. Cyclic voltammetry was used to examine the oxide formation and reduction at the metal surfaces of the PANI/metal composites. After immersing the composite

22

in a solution of 1 M KOH, the potential was cycled between -0.7 V and +0.7 V vs. Ag/AgCl at a scan rate of 100 mV/sec, until steady state was reached.

2.4.2 Propanol oxidation in alkaline solution

The catalytic activity of all composites was examined using propanol oxidation in alkaline solution. The responses of PANI/Au and PANI/Pd were studied first to determine the electrochemical behavior of each metal individually. These data were then compared to the responses of the bimetallic composites to determine if the metals were interacting within the polymer. Metal interaction could result in the formation of a range of electrochemically distinct sites within the polymer, a higher catalytic activity, and changes in poisoning of the catalyst surface. Alcohol oxidation was performed in a solution of 1 M n-propanol and 1 M KOH using cyclic voltammetry with the same parameters from section 2.4.1.

Chapter 3 – Electrochemistry of PANI/Au and PANI/Pd Composites

3.1 Introduction

A thorough understanding of the deposition, morphology, and electrochemistry of PANI/Au and PANI/Pd single metal composites is important in the preparation and characterization of the physical and chemical properties of PANI/Au-Pd bimetallic composites. Linear sweep voltammetry is utilized to control the uptake, dispersion, and content of metal species in the polymer. The resulting voltammetry was evaluated to determine how deposition changes with each subsequent scan, and how metal-polymer interactions differ between Au and Pd. In addition, the morphologies and compositions of the composites were examined using SEM/EDS analysis. Metal oxide formation and reduction was used to evaluate the electrochemically active surface area of the metals within the polymer, and elucidate information about electrochemical processes for the PANI/Au and PANI/Pd composites. Finally, each composite was used as a catalyst for propanol oxidation in alkaline solution to determine each metal's catalytic activity for the process and the extent of surface poisoning for each metal.

3.2 Electrochemical Reduction of Metal Precursors in PANI

The reduction of metal species $PdCl_4^{2-}$ and $AuCl_4^-$ can be expressed using the following electrochemical reactions:

$$PdCl_4^{2-} + 2e^- \rightleftharpoons Pd(0) + 4Cl^- \qquad \textbf{Equation 1}$$

$$AuCl_4^- + 3e^- \rightleftharpoons Au(0) + 4Cl^- \qquad \textbf{Equation 2}$$

The $PdCl_4^{2-}$ anion is known to complex with water, producing hydrated species with the form $PdCl_n(H_2O)_{4-n}{}^{2-n}$ (n=0-4), with $PdCl_4^{2-}$ being the most stable complex.[60] For the purpose of this

study it will be assumed that the primary reacting species is $PdCl_4^{2-}$. In contrast, the $AuCl_4^-$ complex has been shown to remain stable for pH values below five.[61] Therefore, speciation is not an issue because the pH value of the $AuCl_4^-$ solution is 2.88.

Metal anion uptake is initiated through oxidation of PANI to maintain charge neutrality, **Figure 7**. The positive charge at quinoid nitrogen sites and negative charge of the metal precursor are important in establishing the electrostatic interactions that influence dispersion of the species into the polymer. Specifically, the polymer is poised at ~1 V to allow electrostatic interactions between the anion metal precursors ($PdCl_4^{2-}$ and $AuCl_4^-$) and the oxidized polymer to form. As the potential is cycled to more negative values the metal is reduced into the polymer and chloride ions are liberated. Re-oxidation of the metal species in the polymer is minimized during subsequent deposition cycles. During the first scan, the metal anion precursors can only interact with the polymer sites through oxidation of nitrogen groups. However, after the first controlled reduction of $PdCl_4^{2-}$ or $AuCl_4^-$ in PANI there are at least two possible sites for further deposition of the metal species. First, the metal precursors can interact with any remaining sites activated during oxidation of the polymer. Alternatively, the metal precursors can interact with existing metal deposits in the polymer that are also oxidized. Deposition at active polymer sites is expected to diminish with each scan and increase at the existing metal sites in PANI. The controlled electrochemical deposition of single metals into PANI was examined as a function of the number of deposition cycles. The pH values of the metal precursor solutions were sufficient that deposition was achieved without the addition of acid (3.85 and 2.88 for 5 mM $K_2PdCl_4$ and $KAuCl_4$, respectively).
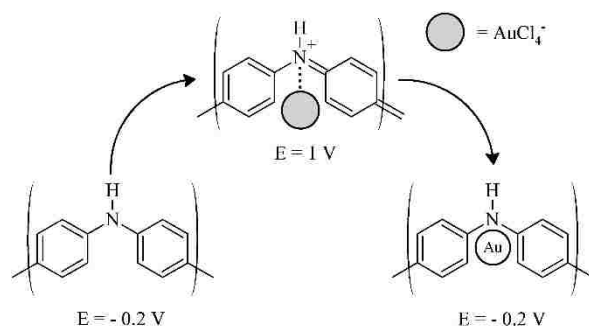
**Figure 7.** Schematic of metal deposition through exploitation of the acid doping mechanism of PANI.

The voltammetric response of a single PANI electrode immersed in 5 mM $PdCl_4^{2-}$ is provided in **Figure 8** (left). The first scan (dashed line) shows the reduction of the metal precursor into pristine PANI is initiated at approximately 0.500 V and reaches a maximum at ~ 0.003 V. The reduction of Pd metal precursor shifts to more negative potential on the second scan (bold line) with diminished current relative to the first. The data indicates that the number of electrostatic sites available within the polymer are reduced with the uptake and reduction of Pd metal after the first scan. The second voltammetric scan is characterized by a decrease in current associated with reduction at electrostatic sites in the polymer. Subsequent Pd deposition is characterized by increasing current at more positive potentials. The deposition is consistent with increasing metal content based on reduction of the anion at existing deposits at 0.260 V for reduction cycles 3-5. The data show that the first scan is predominantly influenced by metal reduction in the pristine polymer. In contrast, more thermodynamically favorable reduction occurs at existing metal deposits at PANI/Pd sites.
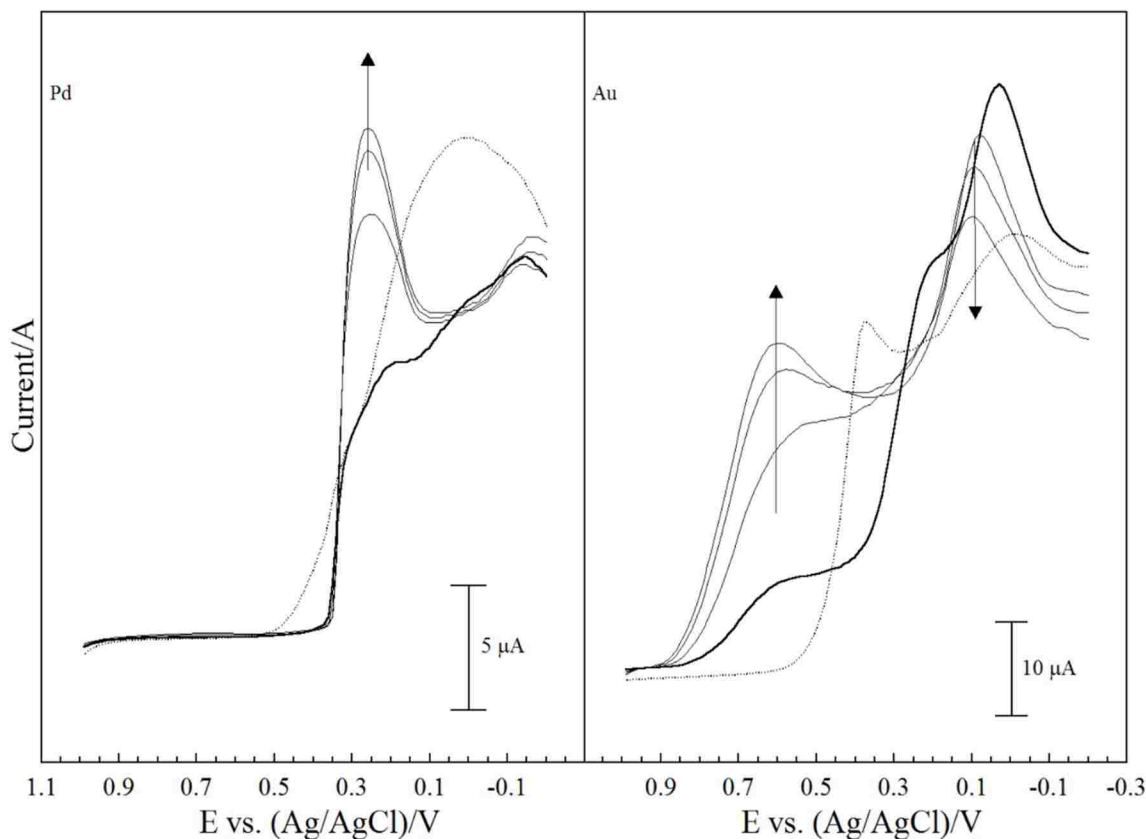
**Figure 8.** Reduction of PdCl$_4^{2-}$ (left) and AuCl$_4^-$ (right) into PANI.   Scans one (dashed), two (bold), and three, four and five (black) are provided.  Arrows indicate the increase or decrease of peaks with increasing scans.

The voltammetric response of a single PANI electrode immersed in 5 mM AuCl$_4^-$ is also provided in **Figure 8** (right).  The figure shows the reduction of the metal precursor into the pristine polymer for the first scan and subsequent reduction cycles into PANI/Au.  The first scan (dashed line) shows two distinct electrochemical reduction processes at ~ 0.375 V and ~ -0.010 V.  The data suggest the initial deposition of Au in PANI occurs at two energetically distinct electrostatic sites in the polymer.  The initial reduction processes shift in opposite directions for the second scan (bold line).  The data suggests that the electrostatic sites in the pristine polymer are influenced by existing Au metal deposits.  The two reduction processes merge into one singe voltammetric wave that decrease with each subsequent scan (3-5).   In addition, a unique voltammetric wave emerges

at ~ 0.600 V and increases with each subsequent reduction of $AuCl_4^-$ into the polymer.  The data is consistent with the increasing metal surface area associated with the accumulation of Au at in the polymer due to reduction at exiting metal deposits.

3.3 SEM/EDS Analysis of PANI/Pd and PANI/Au

The morphology and composition of PANI, PANI/Pd, and PANI/Au composites were examined using SEM/EDS analysis in **Figure 9**.  The SEM image for PANI shows polymer strands with average diameter of $116 \pm 21$ nm.  The porous structure provides a three-dimensional template with a high surface area for metal deposition.  The corresponding EDS spectrum shows the presence of $Cl^-$ in the polymer.  The inclusion of $Cl^-$ comes from the acid doping with $HClO_4$ during the synthesis.  There are two possible explanations for the presence of $Cl^-$.  First, it could be electrostatically bound to the polymer from the reduction of the metal precursor.  Alternatively, it is possible that $Cl^-$ ions are physically trapped inside the polymer matrix from the synthesis of the polymer in the presence of $ClO_4^-$.

For comparison, the SEM image of PANI/Pd after five deposition scans is presented in **Figure 9**.  The image shows that the Pd metal encapsulates PANI, increasing the overall diameter to $210 \pm 26$ nm, with some Pd aggregation on the strands which is consistent with previous studies.[62,63]  The EDS spectrum for PANI/Pd shows that $Cl^-$ is again present in the polymer.  However, the contribution most likely comes from the reduction of the Pd metal precursor and liberation of $Cl^-$ rather than acid doping by $HClO_4$.  The metal deposition is performed in solution that contains only 5 mM $PdCl_4^{2-}$ and any residual $ClO_4^-$ that may be electrostatically bound to the polymer is expelled during the negative scan.  In addition to the $Cl^-$ peak, small Pd peaks emerge relative to the PANI sample at ~2.8 keV and 3.0 keV.[64]
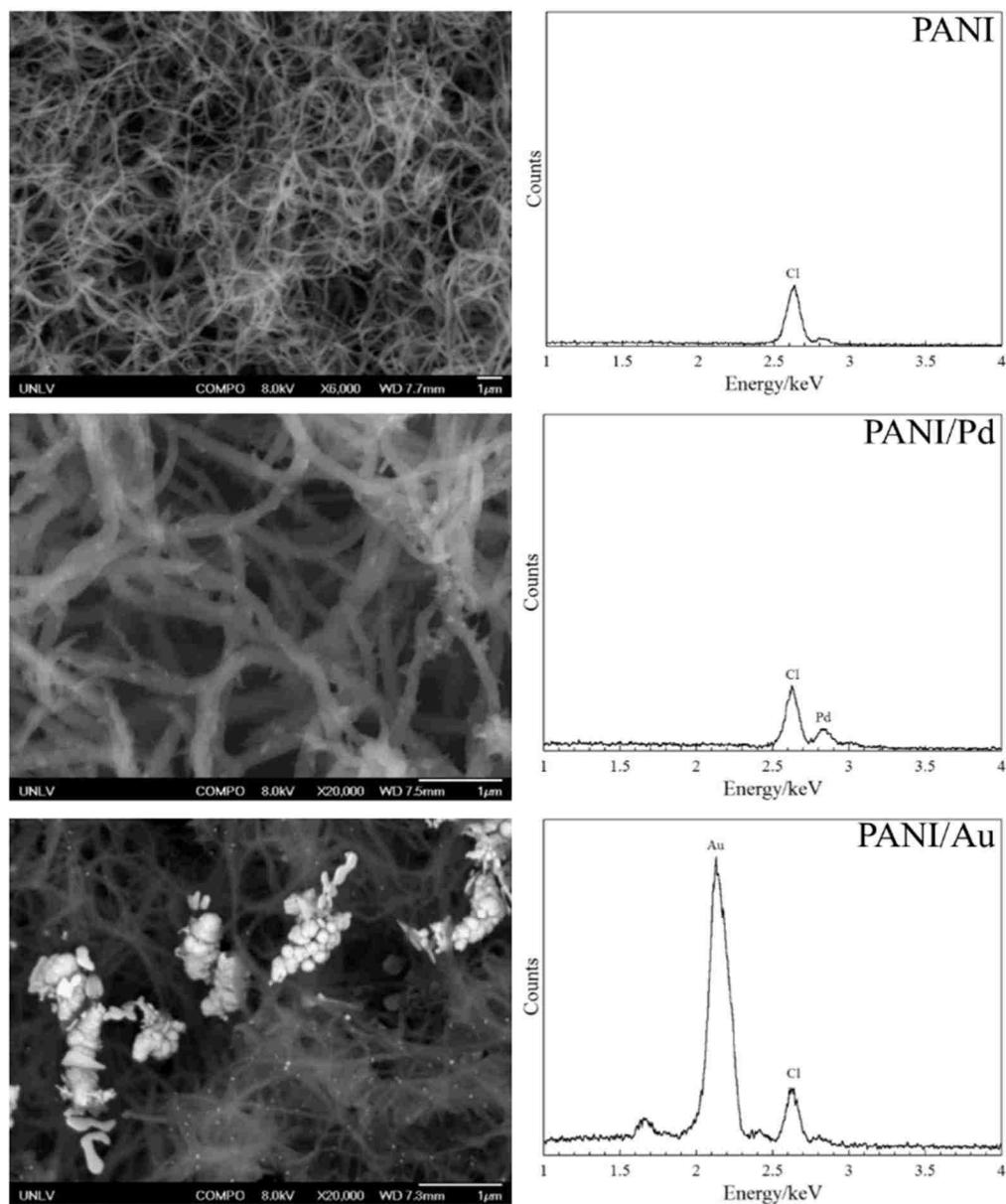
**Figure 9.** SEM images (left) and EDS spectra (right) of pristine PANI (top), PANI/Pd (middle), and PANI/Au (bottom). PANI/Pd and PANI/Au were examined after five metal reduction scans.

In contrast, the SEM image of PANI/Au composites produced after five metal deposition scans shows the formation of 1-2 μm long Au deposits that are comprised of smaller aggregates. In addition, there are 10-50 nm Au particles dispersed throughout the polymer that do not form aggregates. The data suggests that there are energetically distinct deposition sites within the

polymer that influence further deposition of the metal and aggregation. For comparison, the EDS spectrum for PANI/Au is provided which confirms the presence of Au at ~2.1 keV.

3.4 Electrochemistry of PANI/Pd and PANI/Au in Alkaline Solutions

The premise that metal uptake in PANI enhances the conductivity without proton doping was explored in alkaline solutions (1 M KOH, pH $\approx$ 14). The conditions were chosen to ensure that the conductivities of the composites are not influenced by proton doping of the polymer. The formation and reduction of metal oxides and the surface specific oxidation of n-propanol was examined for both PANI/metal composites. The goal was to provide a measure of the electrochemical activity of Au and Pd metals embedded in undoped PANI. The scope of the analysis is focused on electrochemical responses rather than a full mechanistic evaluation of the oxide formation/reduction or the oxidation of propanol at the different metal surfaces. However, electrochemical data derived from metal oxide reduction is used to provide an estimate of the metal surface areas for each species in the polymer. Finally, the surface area derived from metal oxide reduction is utilized with data for the oxidation of propanol to evaluate changes in the charge density (C/cm$^2$) for PANI/metal composites as a function of metal deposition cycle. The electrochemical analysis is presented for the first, third and fifth deposition for both metals in PANI for clarity.

3.4.1 Electrochemistry of PANI/Pd and PANI/Au in Hydroxide

The electrochemical activity of the Pd deposits in PANI were evaluated in 1 M KOH solutions. The voltammetric response was consistent with previous studies that have shown the formation of PdO in alkaline solution is a multi-step process that involves the oxidative adsorption of two hydroxide ions and the loss of water[65,66], **Equation 3**.
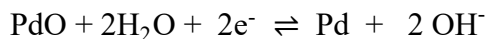
$$PdO + 2H_2O + 2e^- \rightleftharpoons Pd + 2OH^- \qquad\qquad \textbf{Equation 3}$$

The voltammetry for PANI/Pd immersed in 1 M KOH after the first, third and fifth metal reduction are provided in **Figure 10**. The sharp cathodic current at -0.439 V in the voltammetric response obtained for the cathodic scan is consistent with the reduction of PdO. The current increases with increasing metal content in the polymer. While the formation of $PdO_2$ is not ruled out, the reduction occurs at potentials between +0.400 and -0.015 V65[65,66], which is not observed in the voltammetric response for the PANI/Pd composite. A Pd disc electrode with known geometric area was used to determine the charge density for the reduction of Pd oxide. The surface area of the disc electrode was determined using the equation $\pi r^2$, where r is the radius of the Pd disc. Surface roughness was not considered, therefore the surface areas determined are a rough estimate used for qualitative analysis. The calculated charge density value was then utilized with the charge obtained from the reduction of PdO in PANI/Pd to estimate the surface area of the Pd metal embedded in the polymer. The charge density is $1.76 \times 10^{-3}$ $C/cm^2$ for the reduction of palladium oxide at a disc electrode (area = $0.0707$ $cm^2$). Similarly, the charges associated with metal oxide reduction for the first and fifth reductions of the metal precursor into the polymer are $4.69 \times 10^{-7}$ C and $3.36 \times 10^{-5}$ C, respectively. An estimate of the Pd surface area in the polymer is obtained by dividing each of these values with the charge density calculated for the disc electrode. Palladium surface areas of $2.66 \times 10^{-4}$ $cm^2$ and $1.91 \times 10^{-2}$ $cm^2$ are obtained for PANI/Pd after the first and fifth reduction of $PdCl_4^{2-}$ into the polymer, respectively. The metal surface area increases by a factor of ~70 in PANI/Pd between the first and the fifth Pd deposition cycles. **Table 3** provides estimates of the Pd surface area after each Pd reduction scan.

**Table 3.** Estimated Pd surface area after each Pd reduction scan, calculated by dividing the charge passed from Pd oxide reduction by charge density from the equivalent process at a Pd disk electrode with known surface area.

| # Pd Deposition Cycles | Oxide Reduction, Charge (C) | Calculated Surface Area (cm$^2$) |
|:---:|:---:|:---:|
| 1 | $4.69 \times 10^{-7}$ | $2.66 \times 10^{-4}$ |
| 2 | $4.28 \times 10^{-6}$ | $2.43 \times 10^{-3}$ |
| 3 | $1.55 \times 10^{-5}$ | $8.81 \times 10^{-3}$ |
| 4 | $2.33 \times 10^{-5}$ | $1.32 \times 10^{-2}$ |
| 5 | $3.36 \times 10^{-5}$ | $1.91 \times 10^{-2}$ |
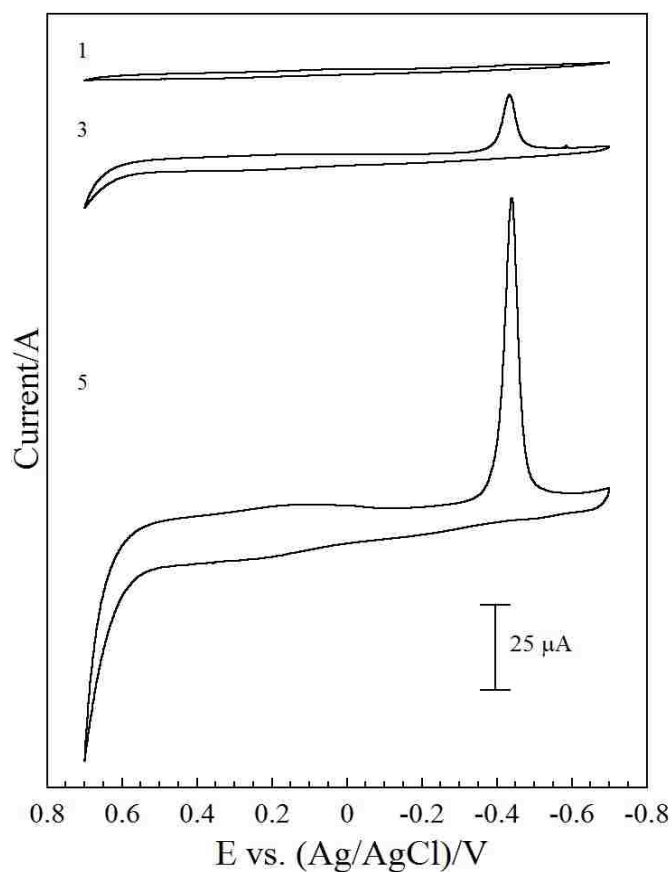


**Figure 10.** The response of a PANI electrode immersed in 1 M KOH after one (top), three (middle), and five (bottom) reductions of PdCl$_4^{2-}$ into the polymer.

The oxidation reaction for the formation of gold oxide in alkaline solution is provided in **Equation 4**. The equation neglects the complex mechanism associated with the adsorption of hydroxide and subsequent formation of gold oxide. However, the voltammetric response of PANI/Au in KOH is consistent with previous studies[67,68] and the overall chemical reaction can be used to provide an estimate of the surface area of Au metal embedded in the polymer. Like Pd, the charge density associated with the reduction of gold oxide at a disc electrode with defined area can be compared with the charge passed for gold embedded in the polymer to estimate the electrochemically active area.

$$Au_2O_3 \; + \; 3\,H_2O \; + \; 6e^- \; \rightleftharpoons 2\,Au \; + \; 6\,OH^- \qquad\qquad \textbf{Equation 4}$$
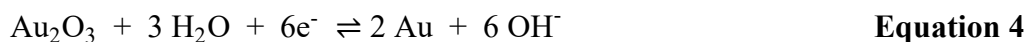
The voltammetry for a PANI/Au electrode immersed in 1 M KOH is provided in **Figure 11** for the first, third, and fifth reductions of $AuCl_4^-$ into the polymer. The voltammetry for the PANI/Au electrodes is consistent with the formation of gold oxide in basic solutions. Although the current associated with the formation/reduction of gold oxide is relatively small after the first reduction of $AuCl_4^-$, the third and fifth reduction show significant increases associated with increasing Au metal content in the polymer. The peak current for formation of gold oxide in PANI/Au is observed at 0.359 V vs. Ag/AgCl during the anodic scan. The reduction of gold oxide occurs at 0.100 V vs. Ag/AgCl during the anodic scan. The data indicate that the electrochemical reduction of $AuCl_4^-$ was used effectively to control and vary the Au metal content in PANI. Furthermore, the formation and reduction of gold oxide is resolved in alkaline solution which confirms the Au metal significantly enhances the electronic properties of the polymer.
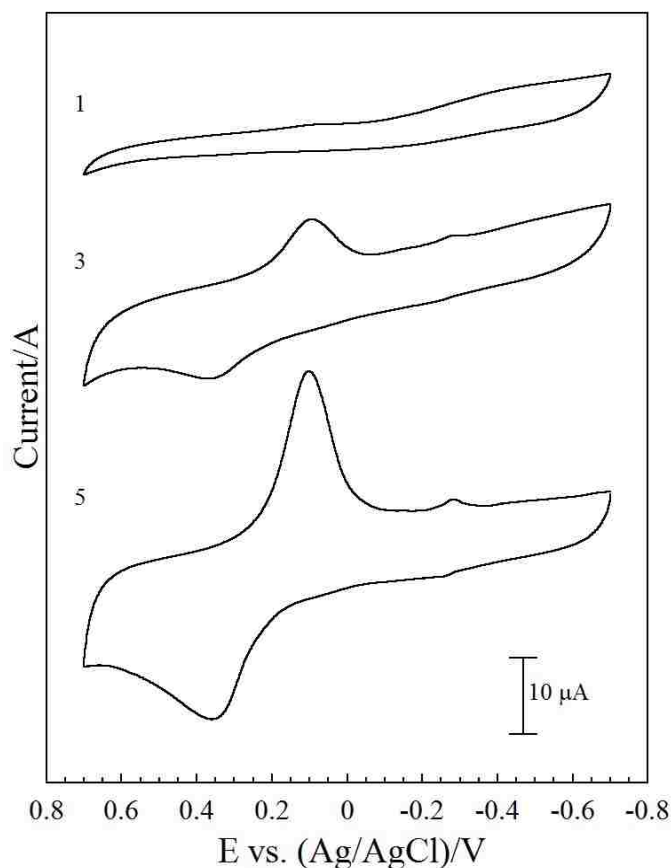
**Figure 11.** The response of a PANI electrode immersed in 1 M KOH after one (top), three (middle), and five (bottom) reductions of $AuCl_4^-$ into the polymer.

The charge density associated with the electrochemical reduction of gold oxide at a disc electrode is used to estimate the active metal surface area in the PANI/Au composite. **Table 4** provides estimates of the Au surface area after each Au reduction scan. The charge density associated with the reduction of gold oxide at an Au disc electrode (area = 0.020 cm$^2$) is 1.38 x 10$^{-3}$ C/cm$^2$. The surface area estimates for Au deposited in the polymer are obtained from the charge associated with metal oxide reduction where Q = 1.90 x 10$^{-6}$ C and Q = 1.92 x 10$^{-4}$ C for the PANI/Au composite after the first and fifth reduction of the metal precursor. An estimate of the gold surface area in the polymer is obtained by dividing each of these values by the charge density calculated for the disc electrode. Gold surface areas of 1.38 x 10$^{-3}$ cm$^2$ and 1.39 x 10$^{-1}$ cm$^2$

are obtained after the reduction of $AuCl_4^-$ into PANI for the first and fifth cycle, respectively. The data indicates that the surface area of Au has increased by two orders of magnitude between the first and fifth reduction of $AuCl_4^-$ into the polymer. The value is much larger than the relative change in surface area estimated for PANI/Pd. The difference might be attributed to the fact that the Pd deposits eventually encapsulate PANI which may minimize the relative change in surface area in comparison to gold.[62] Although the relative gain in Pd surface area is smaller than Au, the data indicates the overall metal surface area can be increased through the sequential electrochemical deposition using the metal precursor.

**Table 4.** Estimated Au surface area after each Au reduction scan, calculated by dividing the charge passed from Au oxide reduction by charge density from the equivalent process at a Au disk electrode with known surface area.

| # Au Deposition Cycles | Oxide Reduction, Charge (C) | Calculated Surface Area $(cm^2)$ |
|:---:|:---:|:---:|
| 1 | $1.90 \times 10^{-6}$ | $1.37 \times 10^{-3}$ |
| 2 | $1.44 \times 10^{-5}$ | $1.04 \times 10^{-2}$ |
| 3 | $3.97 \times 10^{-5}$ | $2.87 \times 10^{-2}$ |
| 4 | $8.49 \times 10^{-5}$ | $6.15 \times 10^{-2}$ |
| 5 | $1.92 \times 10^{-4}$ | $1.39 \times 10^{-1}$ |

3.4.2 Electrocatalytic Oxidation of n-Propanol using PANI/Pd and PANI/Au

The electrochemical response of metal deposited in the polymer can also be probed using propanol oxidation. The general reaction for the oxidation of propanol at a metal surface is given in **Equation 5**.[69,70]

$$CH_3CH_2CH_2OH + 18\,OH^- \longrightarrow 3\,CO_2 + 13\,H_2O + 18\,e^- \qquad \textbf{Equation 5}$$
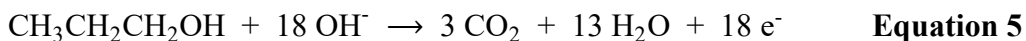
The equation ignores intermediate processes and the possible incomplete oxidation of species at the catalytically active metal surface. However, studies have examined the extent of catalytic electro-oxidation of alcohols at Au and Pd surface. One study[71] determined the final products of oxidation of glycerol in alkaline solution at Au and Pd catalysts using *in situ* infrared spectroscopy. The data suggested that oxidation does not reach completion at either metal. In fact, oxidation at Pd ended with the glycerate ion and Au ended either at glycerate or hydroxypyruvate ion. Without a more detailed analysis of the reaction species generated from the oxidation of propanol the reaction the extent of the reaction based on **Equation 5** is unknown. A full evaluation of solution and surface species from the oxidation of propanol at the PANI/metal composites is beyond the scope of this manuscript. Therefore, the total charge derived from the oxidation of propanol is simply used qualitative tool for comparison of the composites rather than a measure of the extent of the reaction. In addition, the oxidation of propanol can be used as an additional surface specific reaction to probe the signatures for both metals deposited in PANI.[72,73]
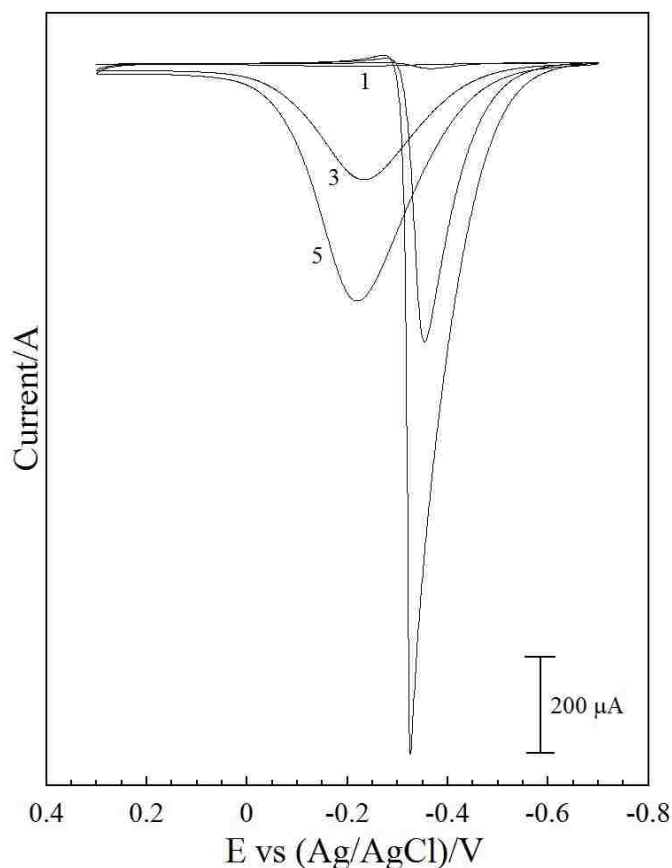
**Figure 12.** Electrocatalytic oxidation of n-propanol using PANI/Pd composites after one, three, and five reductions of Pd.

The oxidation of propanol at PANI/Pd electrodes after the first, third, and fifth reduction of $PdCl_4^{2-}$ in PANI is provided in **Figure 12**. These are the same electrodes used to examine palladium oxide formation/reduction in **Figure 10**. The cathodic and anodic scans for the oxidation of propanol for PANI/Pd are very different; however, the charges associated with propanol oxidation for the anodic and cathodic scans are approximately equal. The potential for the oxidation of propanol is exceeded on the cathodic scan because it occurs only after the reduction of surface adsorbed species or oxide at -0.280 V. The oxidation of propanol is centered at -0.325 V on the cathodic scan, increasing in intensity as a function of increasing Pd in the polymer. In contrast, the anodic scan shows oxidation of propanol over a much larger potential

37

range between -0.555 V to 0.040 V, and is centered at -0.220 V.  The higher current associated with the oxidation of propanol on the cathodic scan indicates that the reaction rate is higher once surface species are reduced from Pd when compared to the anodic scan.  The charge associated with propanol catalysis for the anodic scan was evaluated for the first and fifth reduction of Pd in the polymer giving values of $1.18 \times 10^{-5}$ C and $1.07 \times 10^{-3}$ C, respectively.  The corresponding charge densities are $4.43 \times 10^{-2}$ C/cm$^2$ and $5.62 \times 10^{-2}$ C/cm$^2$ for the catalytic oxidation of propanol once the surface areas of Pd are considered.  **Table 5** summarizes the charge density of propanol oxidation at the PANI/Pd catalyst after each Pd reduction scan.  The charge density reaches a maximum after the third reduction of Pd into PANI then decreases slightly.  The results indicate that the controlled electrochemical reduction of the Pd metal precursor is an effective method for increasing the overall Pd metal content in PANI.  However, the efficiency associated with the increased surface area of the Pd deposits does not increase after the third reduction scan.  The electrochemical data also confirm that the inclusion of Pd in PANI allows the polymer to be utilized in alkaline solutions that preclude acid doping.

**Table 5.** Charge passed and estimated charge density for propanol oxidation at PANI/Pd catalyst after each Pd reduction scan.

| # Pd Deposition Cycles | Charge (C) | Charge Density (C/cm$^2$) |
|---|---|---|
| 1 | $1.18 \times 10^{-5}$ | $4.43 \times 10^{-2}$ |
| 2 | $1.36 \times 10^{-4}$ | $5.59 \times 10^{-2}$ |
| 3 | $5.58 \times 10^{-4}$ | $6.34 \times 10^{-2}$ |
| 4 | $8.33 \times 10^{-4}$ | $6.30 \times 10^{-2}$ |
| 5 | $1.07 \times 10^{-3}$ | $5.62 \times 10^{-2}$ |

The oxidation of propanol for PANI/Au electrodes after the first, third, and fifth reduction of AuCl$_4^-$ in PANI is provide in **Figure 13**. The data is obtained with the same electrodes used in **Figure 11** for the gold oxide formation/reduction. The data show that there is disproportionate oxidation of propanol at PANI/Au for the anodic and cathodic scans. Specifically, the oxidation of propanol is significantly diminished for the cathodic scan relative to the anodic scan. The data from **Figure 11** indicate that oxidation of gold occurs on the anodic scan for the PANI/Au electrode immersed in only 1 M KOH, and that the oxide reduction is initiated at 0.350 V. Therefore, the oxidation of propanol is hindered on the cathodic scan prior to the reduction of surface species.
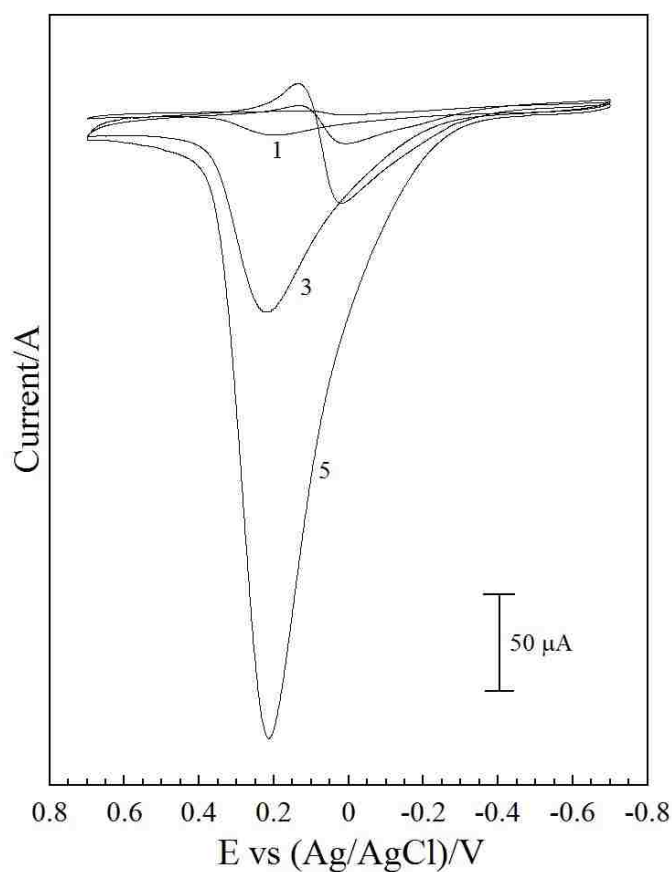


**Figure 13.** Electrocatalytic oxidation of n-propanol using PANI/Au composites after one, three, and five reductions of Au.

To be consistent with the PANI/Pd analysis, the catalytic efficiency of PANI/Au as a function of $AuCl_4^-$ reduction cycles was estimated. **Table 6** summarizes the charge density of propanol oxidation at the PANI/Au catalyst after each Au reduction scan. The charge passed during propanol catalysis is $5.20 \times 10^{-5}$ C and $2.01 \times 10^{-3}$ C after the first and fifth reduction of Au in the polymer. The catalytic charge densities are calculated for the two composites giving values of $3.78 \times 10^{-2}$ C/cm$^2$ and $1.45 \times 10^{-2}$ C/cm$^2$, respectively. The data indicate that the charge density associated with the oxidation of propanol does not increase proportionally with the increase in Au surface area observed for the PANI/Au composites. The oxidation of propanol becomes less efficient as the Au content in the polymer is increased. This loss in efficiency may be an artifact of Au metal aggregation and the formation of large dimension particles. The data provide confirmation of the electrochemical activity of PANI/Au composites in alkaline solutions. Furthermore, the inclusion of Au metal in PANI allows the oxidation of propanol to be probed in alkaline solutions that are traditionally precluded using the polymer.

**Table 6.** Charge passed and estimated charge density for propanol oxidation at PANI/Au catalyst after each Au reduction scan.

| # Au Deposition Cycles | Charge (C) | Charge Density (C/cm$^2$) |
|---|---|---|
| 1 | $5.20 \times 10^{-5}$ | $3.79 \times 10^{-2}$ |
| 2 | $2.18 \times 10^{-4}$ | $2.09 \times 10^{-2}$ |
| 3 | $4.79 \times 10^{-4}$ | $1.67 \times 10^{-2}$ |
| 4 | $8.50 \times 10^{-4}$ | $1.38 \times 10^{-2}$ |
| 5 | $2.01 \times 10^{-3}$ | $1.45 \times 10^{-2}$ |

3.5 Conclusion

The controlled reduction of metal precursors $AuCl_4^-$ and $PdCl_4^{2-}$ to form PANI/metal composites with variable metal content was demonstrated. The uptake and dispersion of the negatively charged metal precursors was initiated through the normal oxidation of PANI. The subsequent reduction of PANI initiated the reduction of the embedded metal precursors to produce metal deposits in the polymer. Initial metal reduction occurred at polymer sites, however after the first reduction, metal deposition at PANI sites decreased and deposition at newly formed PANI/metal sites increased with each subsequent scan. The reactivity of the metal deposits in PANI were examined electrochemically using controlled, surface specific reactions, including metal oxide formation/reduction and the oxidation of n-propanol. The data confirm that the incorporation of Au and Pd metal significantly enhanced the electronic properties of the polymer such that proton doping was not required to maintain the conductivity in alkaline solutions. Both PANI/metal composites remain electrochemically active in alkaline solutions that preclude the proton doping of the polymer. The unique response of each metal to the oxidation of n-propanol can be used to characterize the response of PANI/Au-Pd bimetallic composites.

## Chapter 4 – Simultaneous Deposition of Pd and Au into PANI

4.1 Introduction

The methods derived in Chapter 3 for the controlled deposition of single metal species in PANI are used for the synthesis of PANI/Au-Pd bimetallic composites. This chapter focuses on the preparation and characterization of PANI/Au-Pd composites from the simultaneous deposition from a solution containing both metals. The simultaneous deposition evaluates competitive deposition processes for gold and palladium, which can influence the overall electronic properties of the composite materials. Moreover, the role of controlled deposition of two metal precursors in metal alloying within PANI is evaluated. Reduction of the metals via linear sweep voltammetry is utilized to control the uptake and reduction of both Pd and Au metal precursors to determine if each metal is deposited independently or co-deposited in the polymer. Likewise, the role of subsequent reduction of competing metal species in the polymer when metal is present is explored. The composition and distribution of the two metals in the composite is evaluated as a function of three different metal precursor solutions (with Au:Pd ratios of 1:1, 1:2, and 2:1) to achieve different metal compositions in the polymer. The composites are characterized using the same methods from Chapter 3 for a direct comparison with the single metal composites and bimetallic composites. The morphology and composition of the composites are examined using SEM/EDS analysis. In addition, metal oxide formation and reduction are used to evaluate the electronic properties of the different metal species present in the polymer. Finally, each composite is evaluated as a catalyst for propanol oxidation in alkaline solution to determine if the controlled formation of bimetallic composites produces catalysts with higher activities and reduced surface poisoning in comparison to their monometallic counterparts.

4.2 Electrochemical Reduction of Metal Precursors in PANI

Traditionally, metal deposition in PANI has been achieved using single metal precursors and controlled or spontaneous reduction processes. Spontaneous reduction is a point of contact process where the metal is reduced using the electron rich environment of the polymer. The deposits aggregate at the surface and little control is afforded in terms of dispersion and overall metal composition. In contrast, the previous chapter demonstrated that electrochemical methods allow the oxidation state of the polymer to be controlled and utilized to disperse metal precursors, which is followed by the reduction of the species to produce the composite material. This work represents the first example of the controlled uptake and formation of bimetallic species in PANI. PANI composites containing bimetallic catalysts have primarily been prepared using pre-formed species that are encapsulated during polymer synthesis.[74,75,76,77] The controlled codeposition of Pd and Au onto indium tin oxide glass (ITO)[78], dendrimer-modified ITO[79], and poly(3,4-ethylenedioxythiophene) (PEDOT)[80] have been studied; however, the controlled simultaneous deposition of bimetallic catalysts in PANI has not been previously evaluated.

The simultaneous electrochemical deposition of Au and Pd into PANI was examined as a function of the number of deposition cycles and the mole ratio of metal precursors. The bimetallic deposition was achieved using the same electrochemical parameters as the single metal species which are discussed in Chapter 3. The electrochemical reduction of Au and Pd in PANI was examined using mole ratios ($AuCl_4^-$:$PdCl_4^-$) of 1:1 (2.50 mM:2.50 mM, denoted 1Au1Pd), 2:1 (3.33 mM:1.67 mM, denoted 2Au1Pd), and 1:2 (1.67 mM:3.33 mM, denoted 1Au2Pd), **Figure 14**. The voltammetry associated with the initial reduction of the two metal precursors in pristine polymer is significantly different in comparison to the single metal Au or Pd deposition. For example, the first metal reduction scan (dashed line) from the precursor solution where the Au concentration is

higher (2Au1Pd) most resembles the reduction of Au into pristine PANI. However, the first peak shifts from 0.375 V to 0.331 V while the second voltammetric wave observed at -0.010 V shifts to a more positive potential at 0.100 V. The potential shifts well exceed the resolution of the potentiostat at ± 5 mV. It is likely that the inclusion of $PdCl_4^{2-}$ influences the reduction of $AuCl_4^-$ into pristine polymer. The difference in the direction for the potential shift for the two reduction processes may be influenced by the combined interactions of the two different metal precursors in PANI. In contrast, the second reduction of Au/Pd shows only a single reduction wave at 0.107 V (solid bold line), which is also consistent with response for scans three through five for deposition of Au. The emergence of a new voltammetric wave for scans three to five is observed at about 0.374 V and is indicative of the increase in metal content in the polymer. The results follow the same general trend observed for the reduction of Au in PANI that show the accumulation of metal as a function of reduction scans. However, reduction potentials are shifted relative to Au or Pd alone suggesting that both metals influence subsequent reduction, which can occur at the polymer, Pd, Au, and/or AuPd sites after the first scan. With each additional scan the metal content increases, further influencing the reduction processes. The question remains whether the properties of the metals deposited in PANI act as individual species or synergistically as an alloy in surface electrochemical reactions.
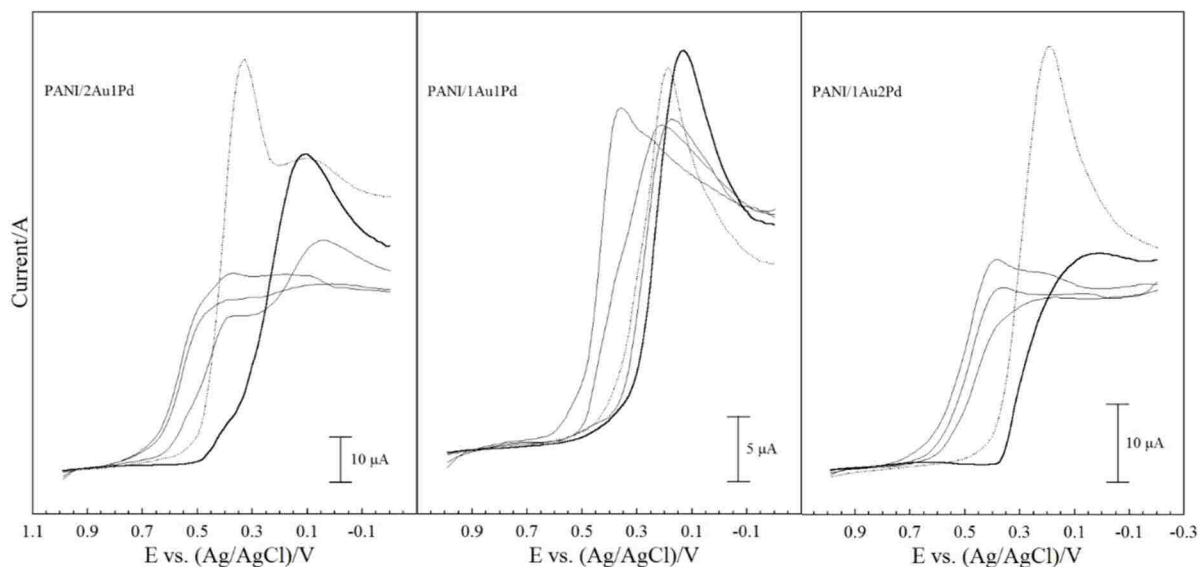
**Figure 14.** Simultaneous reduction of $PdCl_4^{2-}$ and $AuCl_4^-$ into PANI from metal precursor solutions composed of 3.33 mM $KAuCl_4$ and 1.67 mM $K_2PdCl_4$ (left), 2.5 mM $KAuCl_4$ and 2.5 mM $K_2PdCl_4$ (middle), and 1.67 mM $KAuCl_4$ and 3.33 mM $K_2PdCl_4$ (right). Scans one (dashed), two (bold), and three, four and five (black) are provided.

For comparison, the voltammetric response of a PANI electrode immersed in a solution of 2.50 mM $AuCl_4^-$ and 2.50 mM $PdCl_4^{2-}$ (1Au1Pd) does not resemble reduction of $AuCl_4^-$ or $PdCl_4^{2-}$ at pristine PANI. A single voltammetric wave associated with reduction of the metal precursors into the pristine polymer is observed at 0.190 V after the first deposition (dashed line). The potential is shifted negative by 0.185 V and 0.141 V in comparison to the reduction of Au and 2Au1Pd in PANI, respectively. Although it is unclear if reduction using the 1:1 mole ratio solution results in the deposition of equal quantities of each metal, it is clear that the processes are shifted to more negative potentials relative to Au alone or the 2Au1Pd mole ratio sample. Furthermore, the reduction of metal precursor shifts to more negative potential on the second scan with slightly increased current relative to the first (bold line). The third, fourth, and fifth deposition scans show a continued decrease in current associated with the reduction around 0.200 V. There is also an increase in current at 0.357 V consistent with increasing surface area associated with deposition at

existing metal sites in the polymer. The voltammetry for scans two through five are consistent with reduction from 2Au1Pd precursor solution. However, the peak associated with deposition at metal sites is shifted negative 0.017 V, due to the decreased Au:Pd ratio in the precursor solution. The variability of the potentials for reduction processes for solutions containing different mole ratios of the two metal precursors suggest again that both species influence the deposition of metal into the polymer.

The voltammetric response of a single PANI electrode immersed in a solution of 1.67 mM $AuCl_4^-$ and 3.33 mM $PdCl_4^{2-}$ (1Au2Pd) is represented by the right voltammogram in **Figure 14**. The first voltammetric scan (dashed line) shows a single reduction peak at 0.193 V that is consistent with the 1Au1Pd precursor solution. However, the second deposition is more consistent with the first voltammetric scan of Pd in PANI in comparison to either the 2Au1Pd or 1Au1Pd samples. After the second voltammetric scan the deposition of metal species on existing deposits is again observed, consistent with the other samples. The increase in current is consistent with increasing metal surface area in the polymer.

The data for all three samples show an increase in metal content as a function of the number of scans. Energetically distinct voltammetry is resolved for the first and second cycles for the three different solutions studied. The data also indicate that the initial deposition of metal species is predominately influenced by PANI. However, after the initial reduction of metal species into the polymer, subsequent reduction is dominated by metal sites that exist within the polymer. Thus, all the samples show an increase in metal surface areas for scans three through five. Based on the potential differences in the reduction processes we would expect the physical and electrochemical properties of the materials to be different.

4.3 SEM/EDS Analysis of PANI/Au-Pd Bimetallic Composites

A study of the morphology of the composites can be used to evaluate differences in the deposition processes for the simultaneous deposition of Au and Pd in PANI.  Data for the deposition of single metals into PANI demonstrate that deposition of Au and Pd are very different. The data demonstrate that Au deposits as particles with subsequent aggregation while Pd almost completely encapsulates the polymer.  The simultaneous deposition of the two metals in PANI is different.  The SEM images and EDS spectra in **Figure 15** provides a comparison of the morphology and composition of the bimetallic PANI composites formed from the simultaneous deposition of Au and Pd using three different mole ratios.  In addition, measurement of the polymer thickness for the samples presented in **Figure 9** in the previous chapter and **Figure 15** are summarized in **Table 7**.
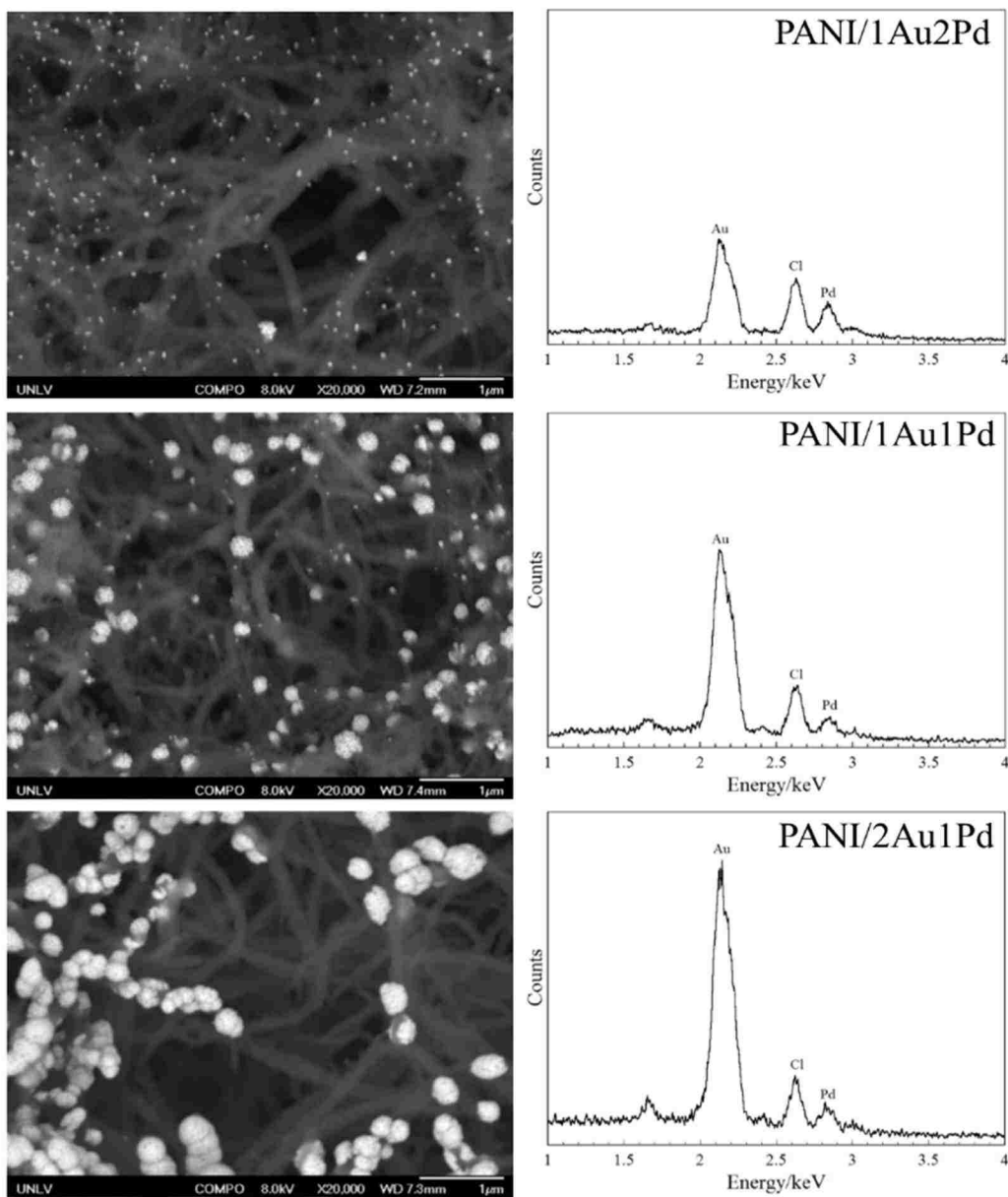
**Figure 15.** SEM images (left) and EDS spectra (right) of PANI/1Au2Pd (top), PANI/1Au1Pd (middle), and PANI/2Au1Pd (bottom).

The average overall diameter of the PANI strands of the PANI/1Au2Pd composite is ~ 171 nm ± 40 nm. While this is still ~ 55 nm wider than pristine PANI, it is less than the ~ 210 nm PANI/Pd strands from Chapter 3. However, with the large standard deviation associated with the thickness measurement, it is possible that the distribution of Pd throughout the polymer is less

uniform than PANI/Pd and strands with the same thickness as PANI/Pd may be present. Alternatively, it can be suggested that the presence of Au affects the Pd deposition mechanism. Competition between the two metals is limited due to the affinity of PANI for Au, which results in its preferential deposition and may minimize encapsulation by Pd. As a result, the PANI/1Au2Pd strands are smaller in diameter in comparison to monometallic PANI/Pd. Also, after the first deposition there are multiple different sites available for metal deposition. Further reduction of the Au and Pd metal precursors can occur at PANI, PANI/Pd, PANI/Au, and sites based on existing Au/Pd deposits. Aggregation will occur if the interaction of the metal precursor with the existing metal deposits is preferential to interaction with PANI. For example, the size and distribution of the Au deposits in the bimetallic sample are likely influenced by the existing Au deposits, the Pd deposits, and the relative concentration of the Pd metal precursor in the solution. In fact, the Au deposits have average diameters of 45 nm ± 9 nm and do not form the large aggregates seen in the PANI/Au sample in Chapter 3. They also appear to be evenly dispersed throughout the polymer. It is important to note that the aggregates, though consistent with aggregates in PANI/Au, may be a mixture of Au and Pd. The corresponding EDX spectrum confirms the presence of both Pd and Au in PANI.

**Table 7.** Size measurements of PANI/metal composites.

| PANI Composite | PANI Thickness (nm) |
|---|---|
| PANI | $116 \pm 21$ |
| PANI/Pd | $210 \pm 26$ |
| PANI/1Au2Pd | $171 \pm 40$ |
| PANI/1Au1Pd | $132 \pm 12$ |
| PANI/2Au1Pd | $154 \pm 40$ |

For comparison, the average thickness of the PANI strands in the PANI/1Au1Pd composite is ~ 20% less than those in the PANI/1Au2Pd composite, which is consistent with the decreased amount of Pd in the metal precursor solution. In contrast, the size of the gold aggregates has increased approximately threefold. Again, it is possible that the aggregates in the SEM image are not all pure Au but alloys of Au and Pd. It is apparent that the concentration change associated with each metal precursor has a direct impact on the morphology of the metal deposits in the polymer. Moreover, the increase in the amount of Au in the composite is corroborated by the EDX spectrum. The intensity of the Au peak increases significantly while the Pd peak shows a slight decrease when compared to the PANI/1Au2Pd composite. Finally, the SEM image for PANI/1Au2Pd composite is provided. The average thickness of the PANI strands is not significantly different from those in the PANI/1Au1Pd composite. The data indicates that the Pd does not necessarily fully encapsulate the polymer as observed for PANI/Pd alone. However, as expected, the size of the Au aggregates continues to increase as the Au concentration in the metal precursor solution increases. The EDS spectrum confirms that the amount of Au present in the sample is increased while the amount of Pd does not change appreciably in comparison.

4.4 Electrochemistry of PANI/Au-Pd Bimetallic Composites in Alkaline Solutions

The electrochemical properties of the composites were examined using metal oxide formation and reduction of the composites as a function of the number of deposition scans. The electrochemical properties of the composites are examined after each metal deposition to evaluate possible alloying during the controlled formation of the bimetallic composites. The bimetallic composites were also examined as possible catalysts for n-propanol oxidation in alkaline solution containing 1 M n-propanol and 1 M KOH. Propanol was chosen for this study because PANI/Au is not an effective catalyst for oxidation of either methanol or ethanol. In addition, the potentials for n-propanol oxidation are distinct for Au and Pd and well documented. The established potentials for the oxidation of n-propanol at Au and Pd allow the contribution of each metal species to be evaluated for the simultaneous deposition of Au and Pd. In addition, the studies may provide information regarding metal interactions and synergistic enhancement of the catalytic properties. Moreover, the voltammetry of the propanol oxidation using bimetallic catalysts can be compared directly to PANI/Pd and PANI/Au to determine if bimetallic composites have higher catalytic activities with reduced surface poisoning when compared to their monometallic counterparts. All composites were examined after five metal deposition scans to ensure a significant amount of each metal is present in the polymer to elucidate the catalytic properties.

4.4.1 Electrochemistry of PANI/Au-Pd Bimetallic Composites in Hydroxide

**Figure 16** presents the metal oxide formation and reduction of the PANI/metal composites synthesized from one metal deposition scan. The top and bottom voltammograms show that Pd oxide reduction and Au oxide reduction occur at -0.439 V and 0.100 V, respectively. The center voltammograms are the responses of the bimetallic composites to oxide formation and reduction. Despite the differences in the compositions of the metal precursor solutions, the peak shapes and

51

peak potentials of all three bimetallic composites are characteristic of PANI/Au oxide formation and reduction. A voltammetric wave corresponding to PANI/Pd is not present. These data suggest that the first deposition results in composites composed primarily of Au. Therefore, it can be concluded that PANI has a much higher affinity for Au than it does for Pd. However, the peak potentials are all shifted negative ~ 0.100 V and the oxide reduction peak is broadened, suggesting that the presence of Pd in the metal precursor solution influences Au deposition.
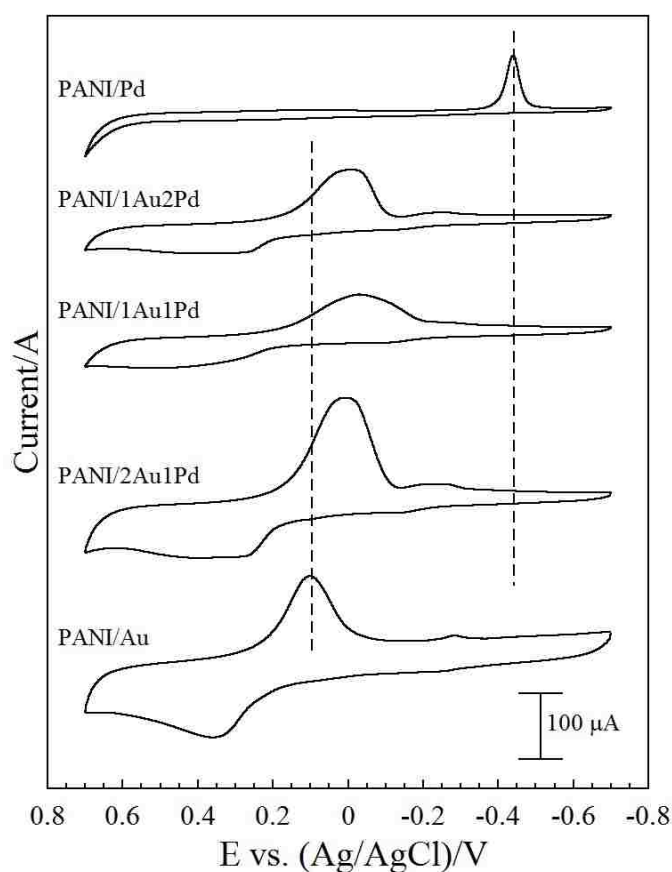


**Figure 16.** The cyclic voltammetric response of a PANI electrode immersed in 1 M KOH after one metal reduction scan from precursor solutions 5 mM $K_2PdCl_4$ (top), 1.67 mM $KAuCl_4$ with 3.33 mM $K_2PdCl_4$ (second), 2.5 mM $KAuCl_4$ with 2.5 mM $K_2PdCl_4$ (third), 3.33 mM $KAuCl_4$ with 1.67 mM $K_2PdCl_4$ (fourth), and 5 mM $KAuCl_4$ (bottom). The corresponding reduction of metal oxide is represented using the dashed lines for single metals Pd and Au for comparison.

**Figure 17** presents the metal oxide formation and reduction of the PANI/metal composites synthesized from five metal deposition scans.  In contrast to the composites in **Figure 16**, the composites in **Figure 17** show multiple energetically distinct metal species.  First, a reduction process is observed for all three bimetallic composites at ~ 0.045 V.  Although there is a slight shift to negative potential when compared to PANI/Au, the process is consistent with the reduction of Au oxide.  Furthermore, there is no electrochemical signature associated with Pd reduction after the first deposition cycle. Each subsequent reduction of metal into PANI results in voltammetry that is consistent with reduction of both Au and Pd metal oxide. For example, the oxide formation and reduction of the PANI/1Au2Pd composite shows there are two overlapping peaks in addition to the Au oxide reduction peak.  Since neither of these processes occur at potentials consistent with PANI/Au nor PANI/Pd, it can be suggested that they are a result of Pd and Au interacting within the polymer, creating multiple electrochemically distinct species.  The first of the overlapping peaks, with a peak maximum at ~ -0.303 V, is most likely due to Pd oxide reduction.  However, the potential shift of ~ 0.136 V compared to PANI/Pd suggests that Au heavily influences the electronic properties of Pd in the polymer.  The second voltammetric wave at ~ -0.190 V occurs at a potential almost exactly halfway between those of PANI/Au and PANI/Pd oxide reductions, suggesting that each metal contributes to the electronic properties.  For comparison, the oxide reduction of the PANI/1Au1Pd composite shows the Pd oxide reduction peak shifts slightly positive and decreases in intensity in response to the decreased Pd concentration and increased Au concentration in the metal precursor solution.  However, the other Au/Pd oxide reduction peak remains relatively unchanged.  In the voltammetric response of the PANI/2Au1Pd composite, the Pd peak continues to shift to a more positive potential, becoming almost engulfed by the Au/Pd peak at ~ -0.182 V.  The positive potential shift of the Pd peak shows the increased influence of

Au as its concentration in the metal precursor solution increases.  The data indicates that controlled simultaneous deposition of Au and Pd forms bimetallic alloys in PANI, and that the chemical and physical properties can be manipulated by varying the composition of the metal precursor in the solution.  The metal surface area cannot be determined for each metal because the contributions of the individual species are convoluted.
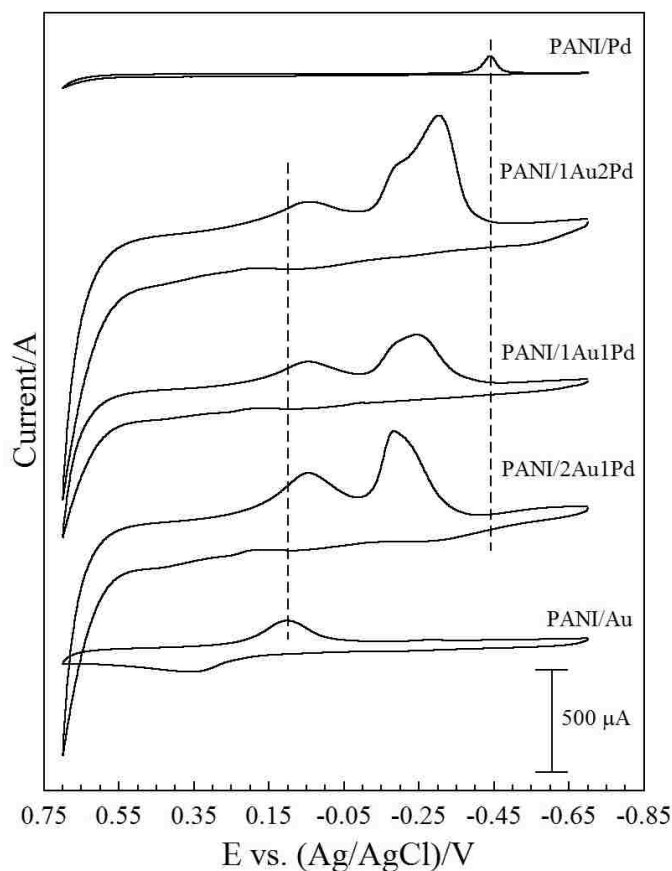


**Figure 17.** The cyclic voltammetric response of a PANI electrode immersed in 1 M KOH after five metal reduction scans from precursor solutions 5 mM $K_2PdCl_4$ (top), 1.67 mM $KAuCl_4$ with 3.33 mM $K_2PdCl_4$ (second), 2.5 mM $KAuCl_4$ with 2.5 mM $K_2PdCl_4$ (third), 3.33 mM $KAuCl_4$ with 1.67 mM $K_2PdCl_4$ (fourth), and 5 mM $KAuCl_4$ (bottom).  The corresponding reduction of metal oxide is represented using the dashed lines for single metals Pd and Au for comparison.

4.4.2 Electrocatalytic Oxidation of n-Propanol using PANI/Au-Pd Bimetallic Composites

The voltammetric responses of the PANI/metal composites in alkaline n-propanol solution are presented in **Figure 18**. All relevant electrochemical measurements are summarized in **Table 8**. The signatures of PANI/Pd and PANI/Au propanol oxidation catalysis is provided for comparison against the PANI/bimetallic composites. First, n-propanol oxidation catalyzed by PANI/Pd produces a symmetrical and broad voltammetric wave at ~ -0.220 V on the anodic scan, while the oxidation on the cathodic scan produces an asymmetrical and sharp voltammetric wave at ~ -0.330 V. For comparison, propanol oxidation catalyzed by PANI/Au produces a broad, symmetrical peak at ~ 0.158 V on the anodic scan, while the cathodic scan shows a very small peak at ~ 0.020 V. It should be possible to determine the level to which each metal contributes to propanol oxidation in the PANI/bimetallic systems because each metal has a unique response.
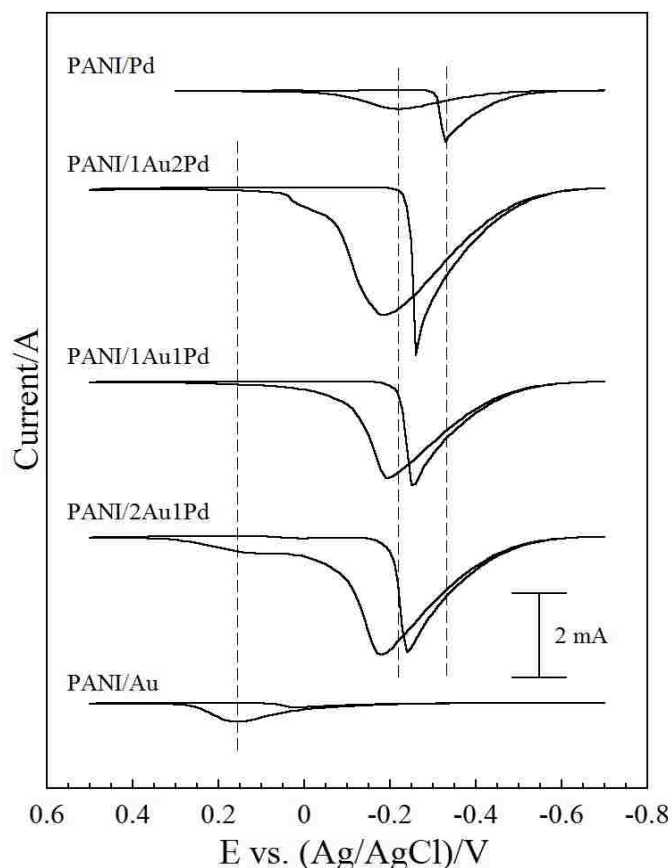
**Figure 18.** The cyclic voltammetric response of a PANI electrode immersed in 1 M n-propanol and 1 M KOH after five metal reduction scans from precursor solutions 5 mM $K_2PdCl_4$ (top), 1.67 mM $KAuCl_4$ with 3.33 mM $K_2PdCl_4$ (second), 2.5 mM $KAuCl_4$ with 2.5 mM $K_2PdCl_4$ (third), 3.33 mM $KAuCl_4$ with 1.67 mM $K_2PdCl_4$ (fourth), and 5 mM $KAuCl_4$ (bottom). The corresponding reduction of metal oxide is represented using the dashed lines for single metals Pd and Au for comparison.

The first bimetallic composite to be examined is PANI/1Au2Pd. The anodic and cathodic scans result in voltammetric waves at ~ -0.187 V ($E_a$) and -0.260 V ($E_c$) respectively. These potentials are shifted slightly positive in comparison to oxidation by PANI/Pd, suggesting that Pd provides a larger contribution to oxidation than Au. In fact, even though the oxide reduction study shows that there is a significant amount of Au metal at the composite surface, there is no signature of oxidation by pure Au present in the voltammogram. However, there is an increase in catalytic activity when compared to monometallic composites.

56

Propanol oxidation at PANI/1Au1Pd and PANI/2Au1Pd show similar results. The peak shapes and potentials are more characteristic of PANI/Pd than PANI/Au. The anodic and cathodic scans for PANI/1Au1Pd result in peaks at ~ -0.195 V and ~ -0.253 V, respectively. The values are slightly different in comparison to the other bimetallic composites. For comparison, the equivalent peaks in the PANI/2Au1Pd composite occur at ~ -0.180 V and ~ -0.242 V for the anodic and cathodic scans, respectively. In addition, it has a voltammetric wave that may be attributed to oxidation by Au species at ~ 0.120 V, which is shifted negative in comparison to PANI/Au (0.158 V). The anodic potential is the same when compared to the results for PANI/1Au2Pd. However, the cathodic potential is shifted even more positive than the other two bimetallic composites. Overall, it appears that Pd influences catalysis more than Au. The positive potential shift indicates that the electrochemical process is more thermodynamically favorable when Au is also present in the polymer.

**Table 8.** Electrochemical measurements from the oxidation of n-propanol in alkaline solution using, PANI/Pd, PANI/1Au2Pd, PANI/1Au1Pd, PANI/2Au1Pd and PANI/Au composites as catalysts.

| PANI Composite | $E_a$ (V) | $E_c$ (V) | $\Delta E$ (V) | $Q_a$ (C) | $Q_c$ (C) | $Q_c/Q_a$ |
|---|---|---|---|---|---|---|
| PANI/Pd | -0.220 | -0.330 | 0.110 | $1.10 \times 10^{-3}$ | $1.21 \times 10^{-3}$ | 1.10 |
| PANI/1Au2Pd | -0.187 | -0.260 | 0.073 | $9.09 \times 10^{-3}$ | $4.93 \times 10^{-3}$ | 0.543 |
| PANI/1Au1Pd | -0.195 | -0.253 | 0.058 | $5.73 \times 10^{-3}$ | $3.54 \times 10^{-3}$ | 0.617 |
| PANI/2Au1Pd | -0.180 | -0.242 | 0.062 | $8.05 \times 10^{-3}$ | $4.29 \times 10^{-3}$ | 0.533 |
| PANI/Au | 0.158 | 0.020 | 0.138 | $1.01 \times 10^{-3}$ | $1.94 \times 10^{-4}$ | 0.191 |

Alcohol oxidation often results in the adsorption of CO, $CO_2$, and other carbonaceous byproducts onto the catalyst, "poisoning" the surface and reducing reactivity due to loss of surface area. The formation of bimetallic catalysts may facilitate the removal of poisoning species from the catalyst surface increasing the efficiency of alcohol oxidation. The peak separation between the cathodic and anodic scans ($\Delta E = E_c - E_a$), and the charge associated with the cathodic and anodic scans ($Q_c/Q_a$) are indicative of the relative efficiency and removal of poisoning species from the metal surfaces.

PANI/Au and PANI/Pd exhibit comparable $\Delta E$ values: 0.138 V and 0.110 V respectively. However, the bimetallic composites have significantly lower $\Delta E$ values, supporting the theory that poisoning species are more easily removed from bimetallic catalysts than from their single metal counterparts. PANI/1Au1Pd has the smallest value (0.058 V), followed by PANI/2Au1Pd (0.062 V) and PANI/1Au2Pd (0.073 V). This phenomenon could be dependent on the size and dispersion of the Au aggregates in PANI. For example, the size of the Au aggregates and amount of Pd present in both the PANI/1Au1Pd and PANI/2Au1Pd composites are similar, as are their $\Delta E$ values. However, the aggregates in the PANI/1Au2Pd are significantly smaller, and there is more Pd present.

To further examine the effects of surface poisoning, the $Q_c/Q_a$ values were compared between PANI/Pd, PANI/Au, and the three bimetallic composites. Propanol oxidation at PANI/Pd was equally efficient in both scan directions, with a $Q_c/Q_a$ value ~ 1. In comparison, oxidation at the PANI/Au catalyst is a relatively slow reaction. Only a small amount of propanol is oxidized after the poisoning species are removed from the electrode surface, resulting in a $Q_c/Q_a$ of 0.191. Once again, the bimetallic composites have $Q_c/Q_a$ values that do not correspond to either PANI/Pd or PANI/Au. PANI/1Au1Pd has the highest value, 0.617. The addition of Au may be slowing

down the reaction, perhaps because there is less Pd at the catalyst surface available for alcohol oxidation. In comparison, PANI/1Au2Pd and PANI/2Au1Pd have $Q_c/Q_a$ values of 0.543 and 0.533 respectively. The reduction in charge for the former is probably due to the delayed removal of poisoning species, while the reduction in charge for the latter is probably due to the reduced availability of Pd sites.

Overall the catalytic activity is enhanced at Au-Pd bimetallic catalysts when compared to PANI/Au and PANI/Pd. The mechanism that leads to the increase is unknown, however there are several possibilities that have been evaluated. First, the voltammetric data are consistent with previous studies[81,82,83] that suggest that Pd is the active site for alcohol oxidation and Au acts as a promoter. For example, Wang et al.[84] proposed that OH⁻ adsorption at Au can promote surface regeneration, which removes surface contaminants from Pd surfaces according to **Equations 6** and **7**:

$$OH_{ads} - Au - Pd - CO_{ads} \; \rightarrow \; Au - Pd - COOH_{ads} \qquad \textbf{Equation 6}$$

$$OH_{ads} - Au - Pd - COOH_{ads} \; \rightarrow \; Au - Pd \, + \, CO_2 \, + \, H_2O \qquad \textbf{Equation 7}$$
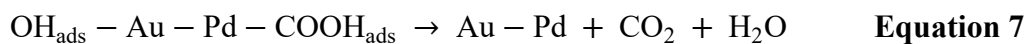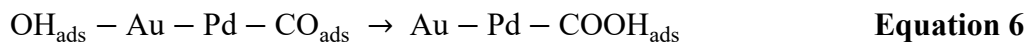
Adsorbed OH⁻ at the Au surface reacts with adsorbed CO at the Pd surface, forming acetate. A second adsorbed OH⁻ reacts with the acetate to form $CO_2$ and $H_2O$, which are desorbed from the catalyst surface. The same study, and others[85,86], also cited an electronic effect, noting that the interaction with Au caused a shift in the d-band center of Pd, which resulted in a stronger methanol adsorption at the alloy surface. A third mechanism involves the stabilization of oxidation intermediates through the bifunctional nature of the catalyst. Rodriguez, et al.[87] propose that the

Au and Pd species form bonds through hydroxyl and alkyl hydrogens, respectively, to stabilize alcohols and facilitate oxidation.

4.5 Conclusion

PANI/AuPd composites can be electrochemically synthesized via the controlled co-deposition of the metals using metal anion precursors.  The electrochemical data demonstrates that the deposition of metal in pristine PANI is energetically distinct in comparison to subsequent reduction when both PANI and PANI/metal sites available. The composition, morphology, and electrochemical properties of the composites can be controlled by varying the concentrations of the two metal precursors in solution.  The differences can be utilized to control dispersion and aggregation of each metal.  The electrochemical formation/reduction of the metal oxides suggests that regardless of the relative concentration of the two metals, deposition of Au is more favorable in the pristine polymer than Pd.  However, after five deposition cycles it is apparent that there are electrochemically distinct sites available, including Au, Pd, and alloyed AuPd bimetallic species. The catalytic oxidation of propanol at bimetallic composites displays higher catalytic efficiency and reduced poisoning when compared to their monometallic counterparts.  The bimetallic composite has higher current associated with the oxidation of propanol on the anodic (positive) scan due to reduced relative poisoning of the metal surface in composites with the single metal. Finally, propanol is oxidized primarily by Pd species.  Therefore, Au either reduces poisoning of the bimetallic catalyst by cleaning the surface or stabilizing the propanol molecule during catalysis.

Chapter 5 – Sequential Deposition of Pd and Au into PANI

5.1 Introduction

Chapter 4 evaluated the role of competition in the alloying of Au and Pd within PANI by depositing the two metals into the polymer simultaneously. In contrast, this chapter will focus on the sequential deposition of Au and Pd into PANI. The influence of metal deposits on the subsequent deposition of a second metal species was investigated. The controlled uptake and reduction of the metal precursors was achieved using linear sweep voltammetry. Electrochemical and SEM/EDS analysis provides insight into the chemical and physical properties of the composites. The goal is to determine if the controlled uptake and reduction of individual metal species sequentially can be used to produce composites with unique or enhanced electrochemical properties relative bimetallic composites produced from controlled simultaneous deposition.

5.2 Electrochemical Reduction of Metal Precursors in PANI

The literature contains few studies evaluating the controlled electrochemical formation of bimetallic catalysts in PANI. Previous studies have evaluated PANI composites formed by sequentially depositing Pt then Ru into the polymer. However, they were unable to form composites in the reverse order because of the inability to deposit Ru into PANI.[88] In addition, the influence of deposition order of Pt and Ag onto a glassy carbon electrode was examined in absence of the polymer.[89] Finally, PANI/Au-Pd composites have been produced using atom by atom deposition.[90] The sequential atomic deposition of Au and Pd was achieved using the normal anion doping of the polymer. Excess metal precursor was removed by washing the PANI membrane with supporting electrolyte. Finally, the metal precursors that remained electrostatically bound in the polymer were reduced. This process was repeated to build the bimetallic catalysts atom by atom in PANI. These three studies thoroughly characterize the

resulting films and evaluate their catalytic activities as a function of amount of metal. However, any data regarding the electrochemistry of the deposition processes themselves was omitted. This study provides a more thorough evaluation of the electrochemistry involved in the controlled uptake and reduction of Au and Pd into PANI/Pd and PANI/Au, respectively.
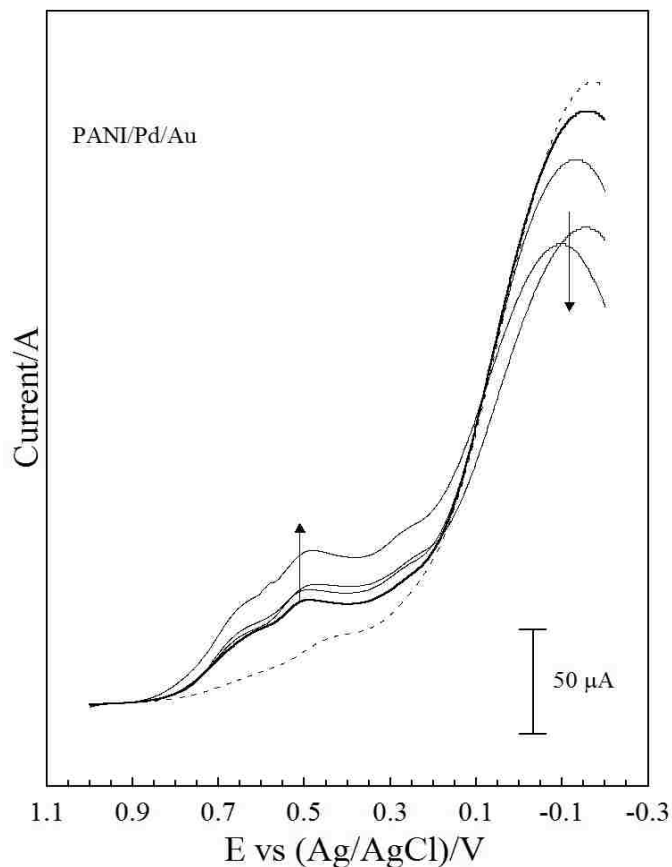


**Figure 19.** Controlled reduction of $AuCl_4^-$ into PANI/Pd. Scans one (dashed), two (bold lines), and three, four, and five (black lines) are provided. Arrows indicate the increase or decrease of current with successive scans.

The voltammetric response of the controlled electrochemical deposition of Au into PANI/Pd is presented in **Figure 19**. The deposition of Au into PANI was explored in Chapter 3. Briefly, the first deposition scan (dashed line) results in the deposition of Au into PANI with two

reduction processes, indicated by voltammetric waves at 0.375 V and -0.010 V. The second scan (bold line) shows that the potentials shift in opposite directions until there is only one distinct deposition wave in PANI after the third scan. In addition, after the first reduction of Au a second voltammetric wave is observed at 0.600 V due to Au deposition at existing metal sites. The deposition of Au into PANI decreases while increasing at PANI/Au with each subsequent scan. It is likely that the oxidation of the polymer is minimized because of the increase in metal content within the PANI/Au composite.

Au deposition into PANI/Pd follows a similar trend with some clear differences. The first scan (dashed line) shows that deposition at PANI sites occurs at a much more negative potential (-0.171 V) when Pd is present in the polymer than when depositing into pristine PANI. Therefore, Pd changes the properties of PANI such that Au deposition at PANI sites becomes less thermodynamically favorable. This may again be an artifact of decreasing electroactive sites within the polymer once Pd is deposited. Deposition of Au at PANI/Pd sites is represented by a small voltammetric wave at 0.413 V which is consistent with metal-on-metal deposition observed previously in Chapter 4. However, the second deposition of Au is initiated about 0.100 V more positive in comparison to the pristine polymer, consistent with deposition at PANI/Au sites. In fact, given the breadth of the metal deposition peak, it is possible that Au can be deposited on several electrochemically distinct sites including Au, Pd, and Au-Pd. As with deposition into pristine PANI, the current associated with deposition at PANI decreases while the current associated with deposition at PANI/metal sites increases with each scan. The data confirm the decrease in PANI sites available as metal content increases.
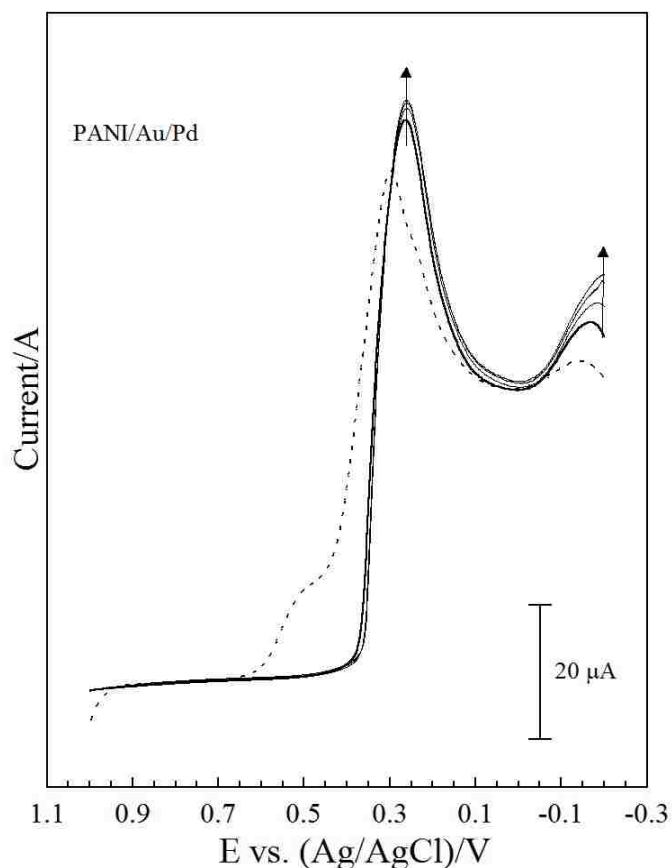
**Figure 20.** Controlled reduction of $PdCl_4^{2-}$ in PANI/Au. Scan one (dashed), two (bold lines), and three, four, and five (black lines) are provided. Arrows indicate the increase or decrease in current with successive scans.

For comparison, deposition of Pd at PANI/Au is presented by **Figure 20**. Previously it was demonstrated that the deposition at PANI occurs at 0.003 V and decreases with each scan. Alternatively, deposition at PANI/Pd sites occurs at 0.260 V and increases with each scan and increasing metal content. The data indicates that Pd deposition occurs primarily at metal sites in PANI/Au. The first deposition (dashed line) is initiated at 0.621 V, with a slight peak at 0.501 V and a peak maximum at 0.297 V. Each subsequent scan contains a peak maximum with a constant current output at 0.263 V and a small peak at about -0.200 V that increases slightly in intensity with each subsequent reduction of Pd. The peak at 0.501 V on the first scan is consistent with Pd

deposition on Au. Deposition at more negative potentials on the second scan occurs at Pd or Au-Pd sites. The peak at -0.200 V could be deposition at PANI shifted significantly negative when compared to deposition at pristine PANI, similar to the shift between deposition of Au at PANI and PANI/Pd sites. However, it is more likely that this peak is due to adsorption of H at the increasing number of Pd sites[91] since the peak increases in intensity with each scan.

5.3 SEM/EDS Analysis of PANI/Au-Pd Bimetallic Composites

The variability in the electrochemical response for the different deposition processes suggests that the deposits formed during the sequential deposition may be different. Specifically, the morphologies of the resulting metal deposits may be very different depending on the order of deposition. The SEM data shown in Chapter 3 demonstrates that Au tends to form aggregates while Pd encapsulates the polymer. The bimetallic composites in Chapter 4 demonstrate that simultaneous deposition of the two metals reduces Pd encapsulation of the polymer and the concentrations of the metal precursors influence the size and distribution of metal particles. The present SEM analysis will be utilized to determine how the presence of one metal in the polymer influences the deposition of a second metal into the same polymer through sequential deposition processes. SEM images of each composite were taken at multiple magnifications to determine the thickness of the PANI strands, the sizes of any metal clusters, and overall distribution of metal throughout the polymer. EDS analysis was also performed to determine the composition of the composites.
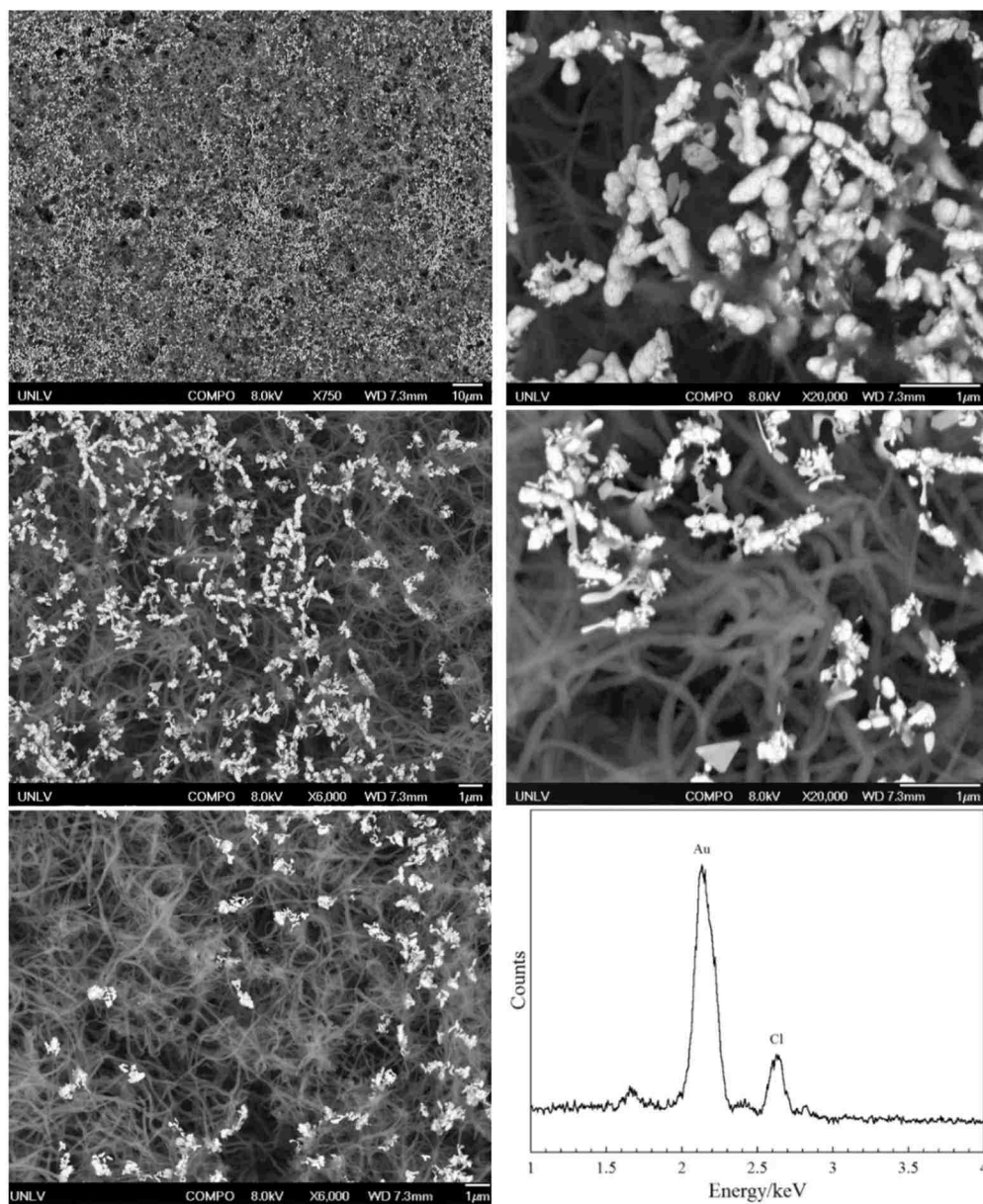
**Figure 21.** SEM images of PANI/5Au/5Pd composite at 750x (top left), 6,000x (middle and bottom left), and 20,000x magnifications (top and middle right), followed by the EDS spectrum (bottom right).

**Figure 21** presents the results of SEM/EDS analysis of the PANI/5Au/5Pd composite.

First, a low magnification view of the polymer at 750x magnification is provided to show the bulk

surface.  It is evident that the metal aggregates do not disperse evenly throughout the polymer.

Rather, the composite is comprised of regions where the aggregates are either clustered together or are sporadically spread, as evidenced at 6,000x magnification. Closer examination of the metal deposits shows that they are consistent in size and shape with those seen in the SEM image of PANI/Au in Chapter 3. Specifically, there are large aggregates made of individual metal particles that encapsulate sections of the polymer as well as two-dimensional deposits that are approximately 500 nm long and vary in shape, consistent with polycrystalline Au deposits.[92,93] However, in contrast to the PANI/Au composite, the 10-50 nm wide metal particles are not present. It is possible that these particles, as well as the PANI strands, are encapsulated by Pd. Interestingly there is no signature of Pd present in the EDS spectrum, despite the increase in PANI strand thickness (116 nm to 150 nm), and the presence of spikes on the strands, which are both consistent with Pd deposition onto PANI. It is possible that the amount of Pd deposited is insignificant in comparison to the amount of Au and $Cl^-$. In fact, the average thickness of the strands is significantly less when compared to PANI/Pd (210 nm vs 150 nm). It is also possible that the presence of Au in PANI significantly hinders the ability of Pd to deposit on the polymer and it is instead depositing preferentially at PANI/Au sites. In Section 5.4.1. the EDS results will be compared to electrochemical studies to produce a more thorough evaluation of the composite's surface composition.
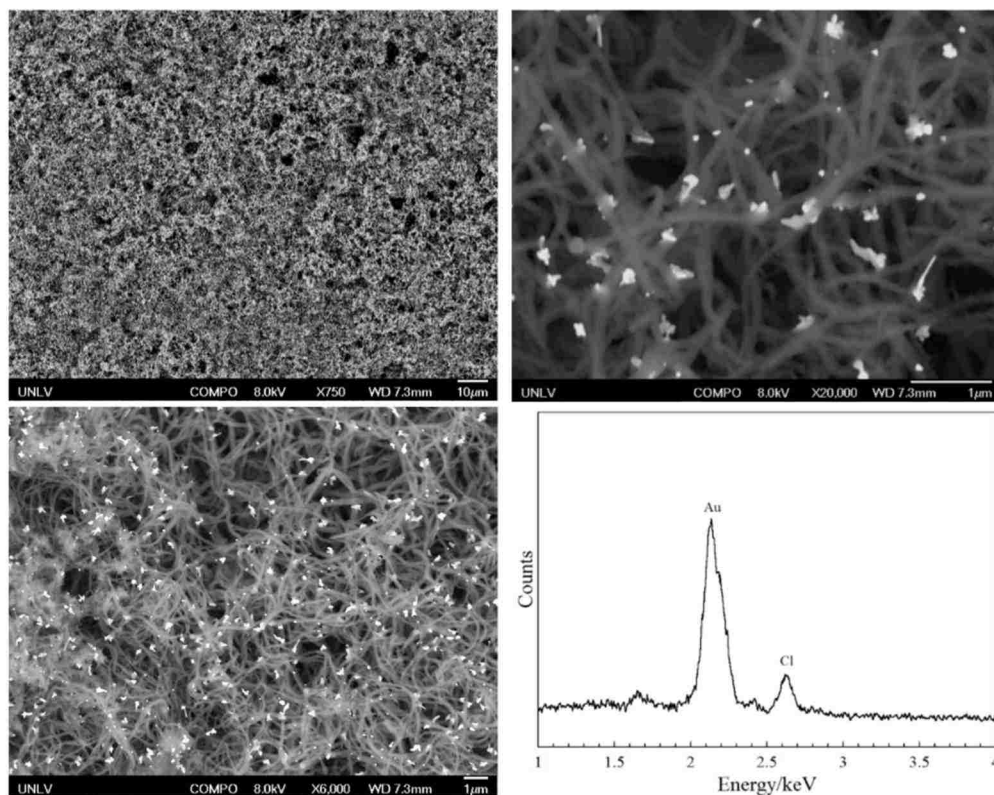
**Figure 22.** SEM images of PANI/5Pd/5Au composite at 750x (top left), 6,000x (bottom left), and 20,000x (top right) magnifications, followed by the EDS spectrum (bottom right).

For comparison, SEM/EDS analysis of the PANI/5Pd/5Au composites are presented in **Figure 22**. At 750x magnification it is apparent that the metal deposits are more evenly distributed throughout the polymer when Pd is deposited before Au. Closer examination of the composites confirms that the metal particles do not cluster in comparison to the PANI/Au and PANI/5Au/5Pd composites. In fact, it is apparent that the presence of Pd in PANI hinders the ability of Au to form large aggregates. Instead, there are small particles ranging from 40 to 120 nm in diameter and metal aggregates about 200 to 500 nm in diameter. Once again, as with PANI/5Au/5Pd, the EDS spectrum does not confirm the presence of Pd, even though the average thickness of the PANI/strands has increased from 116 nm for pristine PANI to 171 nm, as seen in **Table 9**. Although, the average thickness is about 40 nm smaller than that for PANI/Pd the difference may

68

not be significant given the high standard deviations of the measurements. It is still possible that Pd alloys with the Au particles during the Au deposition scans to form the small metal aggregates. However, the electrochemical characterization of the metal deposits is required to determine the relative activity of each metal species and any possible synergistic behavior.

**Table 9.** Thickness of PANI strands for PANI and PANI/metal composites. The PANI/Pd composite was imaged after 5 deposition scans in $K_2PdCl_4$. The bimetallic composites were imaged after 5 deposition scans each in $K_2PdCl_4$ and $KAuCl_4$.

| PANI Composite | PANI Thickness (nm) |
| --- | --- |
| PANI | $116 \pm 21$ |
| PANI/Pd | $210 \pm 26$ |
| PANI/5Au/5Pd | $150 \pm 26$ |
| PANI/5Pd/5Au | $171 \pm 48$ |

5.4 Electrochemistry of PANI/Au-Pd Bimetallic Composites in Alkaline Solutions

The electrochemical properties of the composites were examined using the characteristic metal oxide formation and reduction and catalytic activity of the composites for propanol oxidation in alkaline media. Chapter 3 determined the unique electrochemistry of PANI/Au and PANI/Pd, which was used in Chapter 4 to determine that the two metals interact within PANI when simultaneously deposited into the polymer. The goal is to determine how individual metal species interact when deposited sequentially, and whether the order of deposition results in composites with unique electrochemical properties. Given the differences in the morphologies of the different composites, it can be assumed that the electrochemical properties of the composites will also differ.

5.4.1 Electrochemistry of PANI/Au-Pd Bimetallic Composites in Hydroxide

The electrochemical characterization of the composites will be achieved by evaluating the potentials for metal oxide formation and reduction. The electrochemical processes will be utilized to determine if the metals act independently or synergistically. The electrochemical responses in 1 M KOH of PANI/5Au/xPd, where x signifies the number of Pd deposition scans (1-5) at a PANI/Au electrode, are presented in **Figure 23**. The responses of PANI/Au and PANI/Pd are provided for comparison. After a single deposition scan of Pd into PANI/Au, a voltammetric wave at -0.463 V appears on the cathodic scan, corresponding to reduction of Pd oxides. For comparison, the small shoulder at -0.246 V can be attributed to reduction of oxide at Au-Pd alloys within the polymer. However, in contrast to the response for simultaneously deposited Au-Pd composites, the potential at which Pd oxide reduction occurs in the PANI/5Au/1Pd composite is the same as the corresponding process in PANI/Pd. Therefore, it appears that the presence of Au has little effect on the electrochemical properties of Pd in the bimetallic composite. The larger response at -0.463 V is most likely due to Pd oxide reduction in the absence of Au. In contrast, the small shoulder at -0.246 V is from the reduction of Pd oxide that encapsulated the Au deposits. The diminished gold oxide reduction confirms that the Au surface area has decreased due to Pd deposition and encapsulation.

**Figure 23.** The left presents the voltammetric responses of PANI metal composites in 1 M KOH. The top CV is the PANI film after 5 deposition scans in KAuCl$_4$. The next three are the same PANI/Au film after 1, 3, and 5 deposition scans in K$_2$PdCl$_4$. The response of a PANI film after 5 deposition scans in K$_2$PdCl$_4$ is provided on the bottom for comparison. The corresponding reduction of metal oxide is represented using the dashed lines for single metals Pd and Au for comparison. The responses of the bimetallic composites are presented in overlay on the right.

Investigating the electrochemistry of the metal oxide reduction of PANI/5Au/xPd as a function of number of Pd deposition cycles provides more insights into the deposition behavior of Pd into PANI/Au-Pd bimetallic composites. As described above, the first deposition scan appears to encapsulate both PANI and PANI/Au sites. In subsequent reduction cycles there is an increase in current at -0.463 V corresponding to PANI/Pd metal oxide reduction due to the increase in Pd metal surface area. A more detailed view of the growth of Pd in the polymer is demonstrated by focusing on the cathodic scan between the potentials 0.400 V and -0.600 V. The voltammetry for

PANI/5Au/1Pd shows a significant shoulder from Au-Pd alloying at about -0.246 V that disappears completely with subsequent reduction cycles. It appears that the bulk of the Pd deposition occurs at Au during the first deposition scan. In contrast, Pd deposition occurs at PANI/Pd for each subsequent scan. However, the data contradicts the EDS results shown in **Figure 21**, with the observation of Au only. The discrepancy is most likely due to a difference in relative abundance between Au and Pd, essentially minimizing the Pd signal below the background. Also, electrochemical studies focus purely on the identity of atoms at the electrode surface, while the high energy electron beam used for EDS analysis penetrates into the sample. The data suggests that the Pd forms a core shell over Au aggregates which results in the detection of bulk Au deposits beneath the thin layer of Pd.

For comparison, **Figure 24** presents the oxide formation and reduction of PANI/5Pd/xAu composites, where x signifies the number of Au deposition scans (1-5) at a PANI/Pd electrode. The responses of PANI/Pd and PANI/Au in 1 M KOH are provided for comparison. The PANI/5Pd/xAu composites have three electrochemically distinct sites that form oxides, denoted I, II, and III. Peak I corresponds to Pd oxide formation and reduction which occurs at -0.455 V in PANI/Pd. The potential shifts positive by 0.005 V after a single addition of Au because of the interaction between the two metals. The potential continues to shift as the Au content increases, reaching a final potential of -0.443 V after five reduction cycles. The voltammetry at 0.050 V (III) can be attributed to gold oxide reduction. Finally, oxide reduction for Au-Pd species (II) is observed at -0.275 V after the first reduction cycle. The data is consistent with previous studies which have shown that oxide reduction in Au-Pd alloys occurs at a potential intermediate to the reduction at bulk Au and bulk Pd.[94,95,96] The potential shifts to the more positive potential of -0.199 V as the Au content increases, which is the midpoint between oxide reduction at Au and at

Pd.  The intermediate potential confirms that there are contributions from both Au and Pd in the
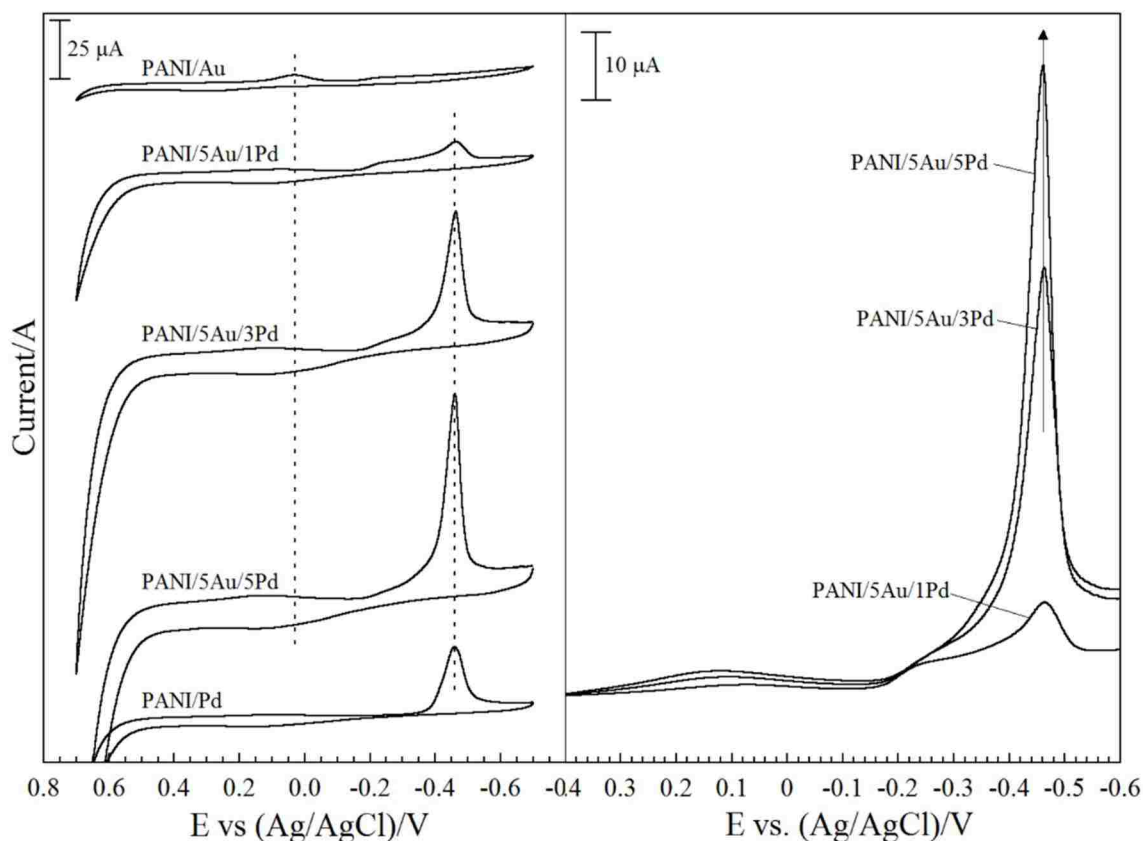
form of alloying.



**Figure 24.** The left presents the voltammetric responses of PANI metal composites in 1 M KOH. The top CV is the PANI film after 5 deposition scans in $K_2PdCl_4$. The next three are the same PANI/Pd film after 1, 3, and 5 deposition scans in $KAuCl_4$. The response of a PANI film after 5 deposition scans in $KAuCl_4$ is provided on the bottom for comparison. The corresponding reduction of metal oxide is represented using the dashed lines for single metals Pd and Au for comparison. The responses of the bimetallic composites are presented in overlay on the right.

The charge passed can also elucidate information about the species at the surface of the

composite.  After the first deposition of Au, the charge associated with oxide reduction at Pd sites,

peak I, is reduced from 5.66 x $10^{-4}$ C to 2.58 x $10^{-4}$ C.    As the Au content increases the charge

remains constant.  In contrast, the charge associated with peak II increases with increasing Au

content. Therefore, Au does not deposit at Pd sites after the first reduction. In addition, the increase in the intensity of peak II is due solely to the increase in the amount of Au in the alloy. However peak III also increases with each addition of Au, so it can be assumed that Au deposits at both alloy sites and Au sites after the first deposition.

5.4.2 Electrocatalytic Oxidation of n-Propanol using PANI/Au-Pd Bimetallic Composites

The use of bimetallic catalysts for propanol oxidation has been shown to increase catalytic activity and to reduce electrode poisoning when compared to the use of their monometallic counterparts. The previous electrochemical studies have shown that the sequential deposition of the metals results in PANI/Au-Pd composites with vastly different morphologies and electrochemical properties than those synthesized using simultaneous deposition. Furthermore, the order of metal deposition has a significant influence on the morphologies and electrochemical properties of the composites. The purpose of this final study is to determine whether PANI/5Au/xPd and PANI/5Pd/xAu also exhibit enhanced electrocatalytic properties relative to previous monometallic and bimetallic composites.
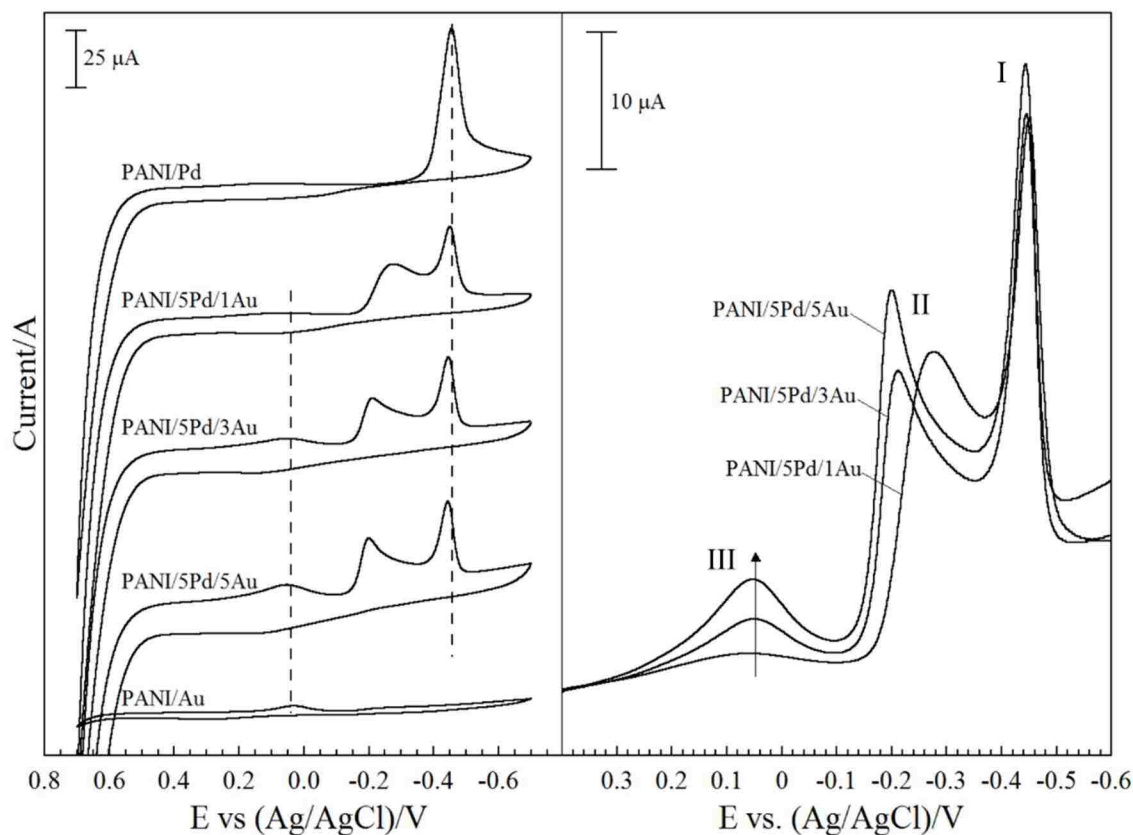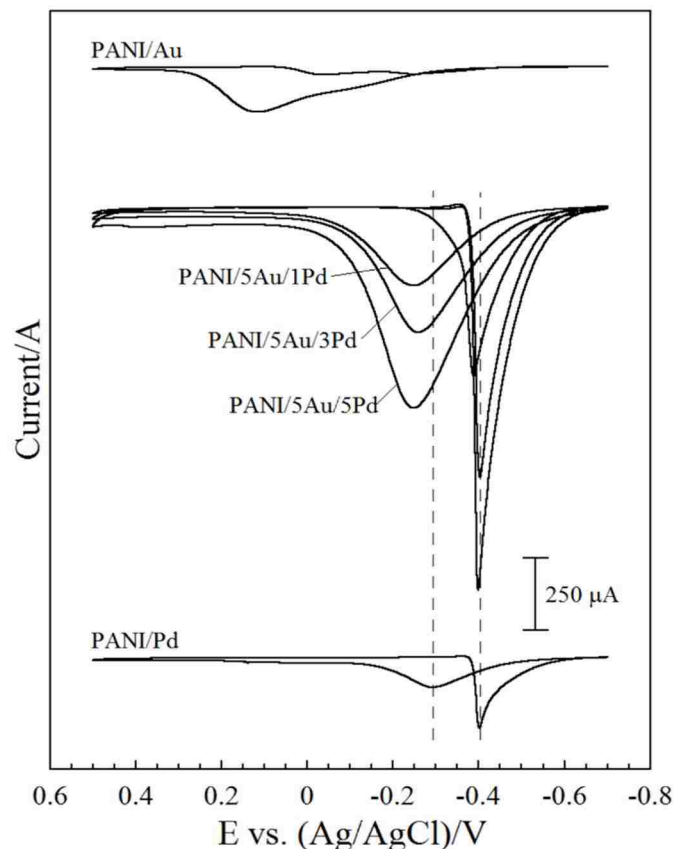
**Figure 25.** Voltammetric response of PANI metal composites in 1 M propanol and 1 M KOH. The top CV is the PANI film after 5 deposition scans in KAuCl$_4$. The next three are the same PANI/Au film after 1, 3, and 5 deposition scans in K$_2$PdCl$_4$. The response of a PANI film after 5 deposition scans in K$_2$PdCl$_4$ is provided on the bottom for comparison. The corresponding oxidation of propanol at single metals Pd and Au is represented using the dashed lines for comparison.

The first composites to be examined are the PANI/5Au/xPd composites, where x signifies the number of Pd deposition scans (1-5) at a PANI/Au electrode. The voltammetric responses of PANI/5Au/1Pd, PANI/5Au/3Pd, and PANI/5Au/5Pd in an alkaline solution of n-propanol are presented in **Figure 25**. Propanol oxidation at the PANI/5Au/xPd catalyst is consistent with oxide formation/reduction. For example, the Au signature disappears, and propanol appears to be oxidized by Pd. As expected, as the number of deposition scans increases, the metal content increases, resulting in a higher charge passed due to the increased amount of alcohol being

oxidized.    Upon closer inspection, however, there are some subtle differences between the PANI/5Au/xPd composites and the PANI/Pd composite. **Table 10** summarizes the peak potentials on the anodic ($E_a$) and cathodic ($E_c$) scans, the potential difference between $E_a$ and $E_c$, and the ratio of the overall charge passed on the cathodic ($Q_c$) and anodic ($Q_a$) scans.

**Table 10.** Electrochemical measurements from the oxidation of n-propanol in alkaline solution using PANI/Au, PANI/5Au/xPd, and PANI/Pd composites as catalysts.

| PANI Composite | $E_a$ (V) | $E_c$ (V) | $\Delta E$ (V) | $Q_a$ (C) | $Q_c$ (C) | $Q_c/Q_a$ |
|---|---|---|---|---|---|---|
| PANI/Au | 0.112 | 0.035 | 0.147 | $5.82 \times 10^{-4}$ | $1.52 \times 10^{-4}$ | 0.261 |
| PANI/5Au/1Pd | -0.248 | -0.388 | 0.140 | $6.49 \times 10^{-4}$ | $6.10 \times 10^{-4}$ | 0.939 |
| PANI/5Au/2Pd | -0.259 | -0.401 | 0.142 | $7.06 \times 10^{-4}$ | $5.49 \times 10^{-4}$ | 0.776 |
| PANI/5Au/3Pd | -0.259 | -0.403 | 0.144 | $1.00 \times 10^{-3}$ | $7.37 \times 10^{-4}$ | 0.734 |
| PANI/5Au/4Pd | -0.252 | -0.400 | 0.148 | $1.46 \times 10^{-3}$ | $9.82 \times 10^{-4}$ | 0.672 |
| PANI/5Au/5Pd | -0.249 | -0.399 | 0.150 | $1.63 \times 10^{-3}$ | $1.07 \times 10^{-3}$ | 0.659 |
| PANI/Pd | -0.291 | -0.402 | 0.111 | $1.16 \times 10^{-4}$ | $1.19 \times 10^{-4}$ | 1.03 |

The potentials at which the oxidation reaction occurs provide insight into the electronic properties of the composites.  For example, the cathodic potential after the first deposition of Pd is indicative of propanol oxidation at Pd alone.  The presence of Au causes the potential to be shifted positive about 0.014 V relative to oxidation at PANI/Pd.  In addition, the anodic potential is shifted positive about 0.043 V relative to PANI/Pd.  It is shifted closer to Au but is otherwise consistent with oxidation at Pd.  These data suggest that Pd encapsulates and minimizes the Au signature after a single deposition.  After the second deposition scan the cathodic and anodic potentials shift negative 0.013 V and 0.011 V, respectively, to values more consistent with

oxidation at Pd. The cathodic potential remains constant as the Pd content is increased. In contrast, the anodic scan shifts back to more positive values after the fourth and fifth depositions. As a result, the anodic and cathodic peak splitting increases from 0.140 V after a single deposition of Pd to 0.150 V after 5 depositions. Both values are larger than the peak splitting associated with oxidation at PANI/Pd, which is 0.111 V. This suggests that a larger driving force is required to remove poisoning species from the PANI/5Au/xPd composites than PANI/Pd. Also, the adsorption of poisoning species becomes prominent and the species are more difficult to reduce from the catalysts as the Pd content increases.

In addition, the charge passed by each composite can be used to evaluate the catalytic efficiency of the composites. Addition of one deposition scan of Pd increases $Q_a$ from 5.82 x $10^{-4}$ C to 6.49 x $10^{-4}$ C. The increase is most likely due to an increase in metal content as opposed to any synergistic effects from the interaction of the two metals. In contrast, $Q_c$ increases four-fold from 1.52 x $10^{-4}$ C to 6.10 x $10^{-4}$ C. This is due to an increase in oxidation occurring at Pd sites. Both $Q_a$ and $Q_c$ increase as the number of Pd deposition scans increase due to an increase in the metal surface. In addition, the $Q_c/Q_a$ values were evaluated to estimate the extent to which the PANI/5Au/xPd composites are affected by surface poisoning. After a single deposition of Pd, the $Q_c/Q_a$ value increases from 0.261 to 0.939. This value is indicative of oxidation of the alcohol at Pd rather than Au. As the amount of Pd content in the composite increases, the value of $Q_c/Q_a$ decreases from 0.939 to 0.659 after five reduction scans for Pd. The contribution of $Q_a$ increases at a faster rate in comparison to $Q_c$. The data suggest that poisoning increases as the Pd metal content increases and the Au deposits are covered. However, overall the bimetallic composites formed from deposition of Pd onto PANI/Au have a higher catalytic activity than either PANI/Pd

or PANI/Au which is an artifact of the increased metal content rather than any synergistic effects

due to the interaction of the two metals.
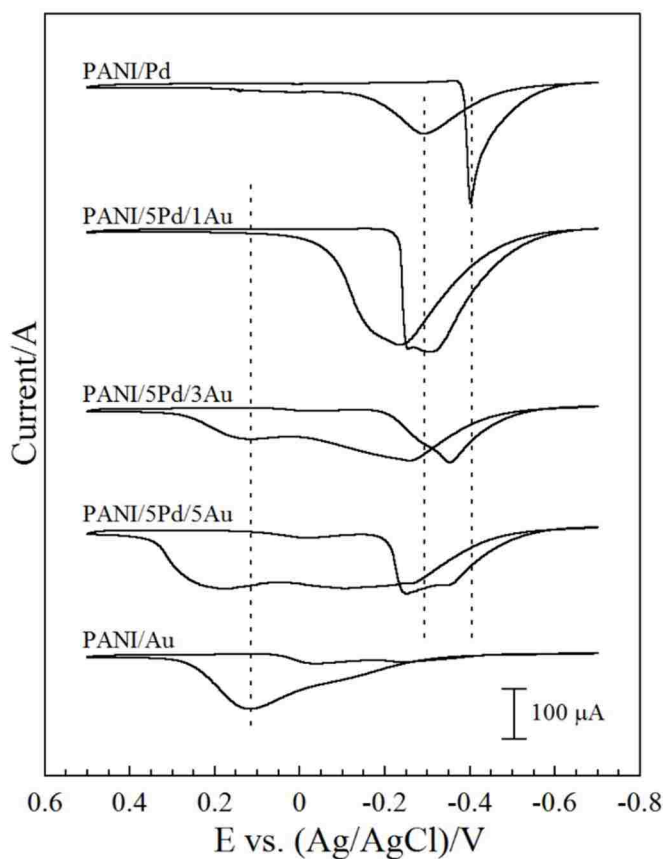


**Figure 26.** Voltammetric response of PANI metal composites in 1 M propanol and 1 M KOH. The top CV is the PANI film after 5 deposition scans in $K_2PdCl_4$. The next three are the same PANI/Pd film after 1, 3, and 5 deposition scans in $KAuCl_4$. The response of a PANI film after 5 deposition scans in $KAuCl_4$ is provided on the bottom for comparison. The corresponding oxidation of propanol at single metals Pd and Au is represented using the dashed lines for comparison.

Evaluation of the voltammetry associated with oxide formation/reduction for the different

composites indicates the order in which the metals are deposited into PANI has a significant effect

on the catalytic behavior of the composite. For example, the voltammetric responses of the

PANI/5Pd/xAu composites in an alkaline solution of n-propanol, where x signifies the number of

Au deposition scans (1-5) at a PANI/Pd electrode, are presented in **Figure 26**. The first obvious difference in the responses of the PANI/5Pd/xAu composites in comparison to the PANI/5Au/xPd composites is the overall shape of the voltammetric waves associated with propanol oxidation. Two overlapping voltammetric waves appear after a single deposition of Au at PANI/Pd. The potentials associated with the oxidation of propanol are consistent with the formation of Pd/Au alloys because they are shifted relative to PANI/Pd or PANI/Au. The oxidation of propanol broadens as the Au content increases due to an increase in alloying with Pd. The data indicates that alloying occurs as Au is reduced into PANI/Pd which does not encapsulate the existing Pd metal deposits.[97] In addition, a voltammetric wave appears at about 0.100 V on the anodic scan after the second deposition of Au, consistent with the formation of distinct PANI/Au sites. The peak increases in intensity and undergoes a positive potential shift with the increase in Au surface area.

**Table 11.** Electrochemical measurements from the oxidation of n-propanol in alkaline solution using PANI/Au, PANI/5Au/xPd, and PANI/Pd composites as catalysts.

| PANI Composite | $Q_a$ (C) | $Q_c$ (C) | $Q_c/Q_a$ |
|---|---|---|---|
| PANI/Pd | $1.16 \times 10^{-4}$ | $1.19 \times 10^{-4}$ | 1.03 |
| PANI/5Pd/1Au | $5.76 \times 10^{-4}$ | $4.38 \times 10^{-4}$ | 0.761 |
| PANI/5Pd/2Au | $4.79 \times 10^{-4}$ | $2.36 \times 10^{-4}$ | 0.491 |
| PANI/5Pd/3Au | $4.33 \times 10^{-4}$ | $1.90 \times 10^{-4}$ | 0.439 |
| PANI/5Pd/4Au | $5.57 \times 10^{-4}$ | $2.50 \times 10^{-4}$ | 0.449 |
| PANI/5Pd/5Au | $7.10 \times 10^{-4}$ | $2.90 \times 10^{-4}$ | 0.408 |
| PANI/Au | $5.82 \times 10^{-4}$ | $1.52 \times 10^{-4}$ | 0.261 |

In addition to overall peak shape, the catalytic activities of the composites were investigated by evaluating the overall charge passed. **Table 11** summarizes the $Q_a$, $Q_c$, and $Q_c/Q_a$ values for the PANI/5Pd/xAu composites. After a single deposition scan of Au at PANI/Pd, the charge passed for the anodic and cathodic scans increase by a factor of 5 and 3.5, respectively. The increase in charge can be attributed to the interaction between Pd and Au. However, the efficiencies of Au, Pd, and the Au-Pd alloys vary as a function of changing composition. Au does not catalyze propanol oxidation as efficiently as the Au-Pd alloys, so as its surface content increases, the overall charge passed by the composite decreases.

In addition, the $Q_c/Q_a$ values were evaluated to determine the composites' susceptibility to surface poisoning. For example, the $Q_c/Q_a$ value after one addition of Au into PANI/Pd decreases from 1.03 to 0.761. This suggests that poisoning species are not reduced as easily from the Au-Pd alloy species as the Au content increases. While the PANI/Pd composite exhibits a higher catalytic activity when Au is reduced into PANI/Pd, the overall efficiency does not increase proportionally. An increase in poisoning due to an increase in Au content is observed.

5.5 Conclusion

The effect of deposition order on the electrochemical properties of PANI/Au-Pd bimetallic composites was explored. Deposition of Pd into PANI/Au appears to occur at a single deposition site. The resulting films contain large Au aggregates separated by regions of PANI and Pd-encapsulated PANI. Despite the lack of Pd signature in the EDS data, the electrochemical data lack the signature of Au, suggesting that the Au could be fully encapsulated in a thin layer of Pd. In contrast, deposition of Au at PANI/Pd occurs at multiple electrochemically distinct sites. The resulting composites have small Au particles evenly dispersed throughout the PANI/Pd film. The electrochemical responses to KOH and n-propanol in KOH show a significant amount of alloying

80

of the two metals. While the catalytic activities of the PANI/5Au/xPd and PANI/5Pd/xAu composites are increased in comparison to monometallic PANI/Pd and PANI/Au, susceptibility to surface poisoning remains an issue.

Chapter 6 – Conclusions

This dissertation evaluates the hypothesis that the controlled uptake and reduction of metal anion precursors is critical in defining both the physical and electronic properties of PANI composites. Moreover, the controlled reduction and deposition of metal species in PANI can result in alloying to produce novel physical and chemical properties that are distinct in comparison to the individual species. First, the method of electrochemical deposition was developed that exploited the normal acid doping mechanism of PANI. Oxidation of the polymer electrode poised in metal precursor solution resulted in the uptake of the metal anion precursor. Reduction of both the polymer and the electrostatically bound metal anion occurred by sweeping the electrode to a negative potential using linear sweep voltammetry. The physical properties of the resulting films were examined using SEM/EDS analysis. Finally, electrochemical studies were used to probe the electrochemical properties of the composites, including the presence of metal alloying, the catalytic activity for propanol oxidation, and the extent of surface poisoning.

The single metal composites PANI/Au and PANI/Pd were studied first to establish the parameters for the controlled uptake, dispersion, and reduction of individual metal species. The studies demonstrated that the potentials at which Au and Pd are reduced into PANI are unique, confirming that PANI/Au and PANI/Pd have distinct chemical properties. The electrochemical properties provided standards against which the bimetallic composites could be compared. SEM data showed that the morphologies were significantly different, with Au forming aggregates and small particles and Pd encapsulating the polymer. The deposition method was used to control the metal deposited and the overall surface area in the composite. The electrochemical characterization of PANI/Au and PANI/Pd in KOH and propanol showed increasing current

responses associated with increasing metal content for both Au and Pd with distinct catalytic activity for propanol oxidation.

The sequential and simultaneous deposition of Au and Pd into PANI were used to evaluate how the controlled reduction of individual species and both species influence the physical and chemical properties of the resulting composites. Specifically, the influence of competitive processes on the overall electronic properties of the materials and any possible alloying of the species within PANI was determined using the two different methods. The electrochemical data demonstrated that the controlled deposition of two metals using both methods followed a similar pattern when compared to individual metal reduction. However, deposition at existing metal sites occurred at a potential intermediate to reduction at PANI/Au and PANI/Pd metal sites.

SEM images suggest that size and dispersion of metal aggregates are influenced by the concentrations of $AuCl_4^-$ and $PdCl_4^{2-}$ in the metal precursor solution for the simultaneous deposition. It was also demonstrated that Au is the primary species deposited on the first reduction scan, regardless of the ratio of Au/Pd concentrations in the metal precursor solutions. The data confirms that PANI has a higher affinity for Au when compared to Pd. The voltammetric response of the composites in KOH after subsequent metal scans reveals three electrochemically distinct sites, including one characteristic of Au oxide reduction, one characteristic of Pd oxide reduction, and one that results from the interaction of the two species, which is attributed to alloying. Moreover, all three bimetallic composites have increased catalytic activity for propanol oxidation and reduced electrode poisoning when compared to PANI/Pd and PANI/Au.

Sequential deposition produces bimetallic composites that are markedly different than those obtained through simultaneous deposition. The sequential deposition of Pd into PANI/Au encapsulates the Au aggregates and particles. The electrochemistry of the resulting composite is characteristic of PANI/Pd. Conversely, Au reduction into PANI/Pd results in small Au particles and Au-Pd alloys. Oxide formation of the PANI/5Pd/xAu composites shows three electrochemically distinct sites corresponding to Au, Pd, and an alloy of the two. Propanol oxidation occurs over a 1 V range because of the multiple distinct Au-Pd alloys within the polymer. Both composites, regardless of deposition order, show an increase in catalytic activity for propanol oxidation relative to PANI/Au or PANI/Pd alone.

The controlled uptake and reduction of Au and Pd in PANI using both simultaneous and sequential deposition was utilized to form bimetallic PANI/Au-Pd composites. Control over the deposition of the metals was demonstrated. Factors such as metal deposit size, dispersion, and surface area were directly influenced using the controlled deposition methods developed in this dissertation. Differences in the morphology of deposits were equated with changes in the electrochemical properties relative to individual metal species in the polymer. Therefore, it can be concluded that the controlled deposition of metal species either simultaneously or sequentially influences the physical and electrochemical properties of the composites. Finally, PANI/Au-Pd bimetallic composites have been shown to have higher catalytic activities for propanol oxidation than either PANI/Pd or PANI/Au with evidence that alloying of the two species contributes to an overall increase in efficiency.

References

[1] X. Chen, L. Shen, C.A. Yuan, C.K.Y. Wong, G. Zhang, Molecular model for the charge carrier density dependence of conductivity of polyaniline as chemical sensing materials, *Sens. Actuators, B* **177** (2013) 856-861.

[2] R. Kumar, B.C. Yadav, Humidity sensing investigation on nanostructured polyaniline synthesized via chemical polymerization method, *Mater. Lett.* **167** (2016) 300-302.

[3] Y. Li, W. Li, H. Zhou, F. Wang, Y. Chen, Y. Wang, C. Yu, A facile method for the sensing of antioxidants based on the redox transformation of polyaniline, *Sens. Actuators, B* **208** (2015) 30-35.

[4] R.M. Bandeira, J. van Drunen, A.C. Garcia, G. Tremiliosi-Filho, Influence of the thickness and roughness of polyaniline coatings on corrosion protection of AA7075 aluminum alloy, *Electrochim. Acta* **240** (2017) 215-224.

[5] B. Yao, G. Wang, J. Ye, X. Li, Corrosion inhibition of carbon steel by polyaniline nanofibers, *Mater. Lett.* **62** (2008) 1775-1778.

[6] H. Bejbouj, L. Vignau, J.L. Miane, T. Olinga, G. Wantz, A. Mouhsen, E.M. Oualim, M. Harmouchi, Influence of the nature of polyaniline-based hole-injecting layer on polymer light emitting diode performances, *Mater. Sci. Eng., B* **166** (2010) 185-189.

[7] H.L. Wang, A.G. MacDiarmid, Y.Z. Wang, D.D. Gebier, A.J. Epstein, Application of polyaniline (emeraldine base, EB) in polymer light-emitting devices, *Synth. Met.* **78** (1996) 33-37.

[8] A.A. Syed, M.K. Dinesan, Review: Polyaniline-A novel polymeric material, *Talanta* **38** (1991) 815-837.

[9] A.J. Heeger, Semiconducting and metallic polymers: the fourth generation of polymeric materials, *Curr. Appl. Phys.* **1** (2001) 247-267.

[10] H. Shirakawa, E.J. Louis, A.G. MacDiarmid, C.K. Chiang, A.J. Heeger, Synthesis of electrically conducting organic polymers: halogen derivatives of polyacetylene, $(CH)_x$, *J. Chem. Soc., Chem. Commun.* (1977) 578-580.

[11] T.V. Vernitskaya, O.N. Efimov, Polypyrrole: a conducting polymer; its synthesis, properties and applications, *Russ. Chem. Rev.* **66** (1997) 443-457.

[12] A.G. Macdiarmid, J.-C. Chiang, M. Halpern, W.-S. Huang, S.-L. Mu, L.D. Nanaxakkara, S.W. Wu, S.I. Yaniger, "Polyaniline": Interconversion of Metallic and Insulating Forms, *Mole. Cryst. Liq. Cryst.* **121** (1985) 173-180.

[13] G.E. Wnek, J.C.W. Chien, F.E. Karasz, C.P. Lillya, Electrically conducting derivative of poly(p-phenylene vinylene), *Polymer* **20** (1979) 1441-1443.

[14] M. Brie, R. Turcu, C. Neamtu, S. Pruneanu, The effect of initial conductivity and doping anions on gas sensitivity of conducting polypyrrole films to NH3, *Sens. Actuators B* **37** (1996) 119-122.

[15] A.G. MacDiarmid, "Synthetic metals": a novel role for organic polymers, *Curr. Appl. Phys.* **1** (2001) 269-279.

[16] H. Bai, G. Shi, Gas Sensors Based on Conducting Polymers, *Sensors* **7** (2007) 267-307.

[17] S. L. Hsu, A. J. Signorelli, G. P. Pez, R. H. Baughman, Highly conducting iodine derivatives of polyacetylene: Raman, XPS, and x-ray diffraction studies, *J, Chem. Phys.* **69** (1978) 106-111.

[18] T.-H. Le, Y. Kim, H. Yoon, Electrical and Electrochemical Properties of Conducting Polymers, *Polymers* **9** (2017) 150.

[19] C. Menardo, M. Nechtschein, A. Rousseau, J.P. Travers, P. Hany, Investigation on the structure of polyaniline: $^{13}C$ N.M.R. and titration studies, *Synth. Met.* **25** (1988) 311-322.

[20] G. Ciric-Marjanovic, Recent advances in polyaniline research: Polymerization mechanisms, structural aspects, properties and applications, *Synth. Met.* **177** (2013) 1-47.

[21] D.W. Hatchett, M. Josowicz, J. Janata, Acid Doping of Polyaniline: Spectroscopic and Electrochemical Studies, *J. Phys. Chem. B* **103** (1999) 10992-10998.

[22] E.M. Geniès, A. Boyle, M. Lapkowski, C. Tsintavis, Polyaniline: A historical survey, *Synth. Met.* **36** (1990) 139-182.

[23] W.-S. Huang, B.D. Humphrey, A.G. MacDiarmid, Polyaniline, a novel conducting polymer. Morphology and chemistry of its oxidation and reduction in aqueous electrolytes, *J. Chem. Soc., Faraday Trans. 1: Physical Chemistry in Condensed Phases* **82** (1986) 2385-2400.

[24] D.W. Hatchett, R. Wijeratne, J.M. Kinyanjui, Reduction of $PtCl_6^{2-}$ and $PtCl_4^{2-}$ in polyaniline: Catalytic oxidation of methanol at morphologically different composites, *J. Electroanal. Chem.* **593** (2006) 203-210.

[25] S. Palmero, A. Colina, E. Muñoz, A. Heras, V. Ruiz, J. López-Palacios, Layer-by-layer electrosynthesis of Pt–Polyaniline nanocomposites for the catalytic oxidation of methanol, *Electrochem. Commun.* **11** (2009) 122-125.

[26] E.C. Venancio, W.T. Napporn, A.J. Motheo, Electro-oxidation of glycerol on platinum dispersed in polyaniline matrices, *Electrochim. Acta* **47** (2002) 1495-1501.

[27] D.W. Hatchett, M. Josowicz, J. Janata, Electrochemical Formation of Au Clusters in Polyaniline, *Chem. Mater.* **11** (1999) 2989-2994.

[28] A.H. Saheb, S.S. Seo, Polyaniline/Au Electrodes for Direct Methanol Fuel Cells, *Anal. Lett.* **44** (2011) 2221-2228.

[29] R.K. Pandey, V. Lakshminarayanan, Ethanol electrocatalysis on gold and conducting polymer nanocomposites: A study of the kinetic parameters, *Appl. Catal. B* **125** (2012) 271-281.

[30] D.W. Hatchett, N.M. Millick, J.M. Kinyanjui, S. Pookpanratana, M. Bär, T. Hofmann, A. Luinetti, C. Heske, The electrochemical reduction of $PdCl_4^{2-}$ and $PdCl_6^{2-}$ in polyaniline: Influence of Pd deposit morphology on methanol oxidation in alkaline solution, *Electrochim. Acta* **56** (2011) 6060-6070.

[31] R.K. Pandey, V. Lakshminarayanan, Electro-Oxidation of Formic Acid, Methanol, and Ethanol on Electrodeposited Pd-Polyaniline Nanofiber Films in Acidic and Alkaline Medium, *J. Phys. Chem. C* **113** (2009) 21596-21603.

[32] M.I. Prodromidis, E.M. Zahran, A.G. Tzakos, L.G. Bachas, Preorganized composite material of polyaniline–palladium nanoparticles with high electrocatalytic activity to methanol and ethanol oxidation, *Int. J. Hydrogen Energy* **40** (2015) 6745-6753.

[33] I. Dodouche, F. Epron, Promoting effect of electroactive polymer supports on the catalytic performances of palladium-based catalysts for nitrite reduction in water, *Appl. Catal. B* **76** (2007) 291-299.

[34] X. Ma, Y. Feng, Y. Li, Y. Han, G. Lu, H. Yang, D. Kong, Promoting effect of polyaniline on Pd catalysts for the formic acid electrooxidation reaction, *Chin. J. Catal.* **36** (2015) 943.951.

[35] S. Beyhan, Electrocatalytic Properties of Au (hkl) Electrodes Towards Oxidation of Ethanol in Alkaline Media, *Int. J. Electrochem. Sci.* **9** (2014) 3259-3268.

[36] X. Wang, B. Tang, X. Huang, Y. Ma, Z. Zhang, High activity of novel nanoporous Pd–Au catalyst for methanol electro-oxidation in alkaline media, *J. Alloys Compd.* **565** (2013) 120-126.

[37] A. Nirmala Grace, K. Pandian, Pt, Pt–Pd and Pt–Pd/Ru nanoparticles entrapped polyaniline electrodes – A potent electrocatalyst towards the oxidation of glycerol, *Electrochem. Commun.* **8** (2006) 1340-1348.

[38] M. Simões, S. Baranton, C. Coutanceau, Electro-oxidation of glycerol at Pd based nano-catalysts for an application in alkaline fuel cells for chemicals and energy cogeneration, *Appl. Catal. B* **93** (2010) 354-362.

[39] J. Fu, K. Yang, C. Ma, N. Zhang, H. Gai, J. Zheng, B.H. Chen, Bimetallic Ru–Cu as a highly active, selective and stable catalyst for catalytic wet oxidation of aqueous ammonia to nitrogen, *Appl. Catal. B* **184** (2016) 216-222.

[40] T.R. Garrick, W. Diao, J.M. Tengco, E.A. Stach, S.D. Senanayake, D.A. Chen, J.R. Monnier, J.W. Weidner, The Effect of the Surface Composition of Ru-Pt Bimetallic Catalysts for Methanol Oxidation, *Electrochim. Acta* **195** (2016) 106-111.

[41] C. Hsu, C. Huang, Y. Hao, F. Liu, Au/Pd core-shell nanoparticles for enhanced electrocatalytic activity and durability, *Electrochem. Commun.* **23** (2012) 133-136.

[42] A.A. Rodriguez, C.T. Williams, J.R. Monnier, Effect of Structure and Substituents in the Aqueous Phase Oxidation of Alcohols and Polyols Over Au, Pd, and Au–Pd Catalysts, *Catal. Lett.* **145** (2015) 750-756.

[43] T. Iwasita, H. Hoster, A. John-Anacker, W. F. Lin, W. Vielstich, Methanol Oxidation on PtRu Electrodes. Influence of Surface Structure and Pt-Ru Atom Distribution, *Langmuir* **16** (2000) 522-529.

[44] N. W. Smirnova, O. A. Petrii, A. Grzejdziak, Effect of ad-atoms on the electro-oxidation of ethylene glycol and oxalic acid on platinized platinum, *J. Electroanal. Chem.* **251** (1988) 73-87.

[45] H. Abdullah, N.M. Naim, A.A. Hamid, A.A. Umar, Characterization and Fabrication of Nanocomposite Thin Films of PANI Embedded with Ag-Mn Alloy for E. coli Sensor, *Mater. Today: Proc.* **3** (2016) 538-544.

[46] G. Sharma, M. Naushad, A. Kumar, S. Devi, M.R. Khan, Lanthanum/Cadmium/Polyaniline bimetallic nanocomposite for the photodegradation of organic pollutant, *Iran. Polym. J.* **24** (2015) 1003-1013.

[47] P. Boomi, H.G. Prabu, J. Mathiyarasu, Synthesis and characterization of polyaniline/Ag–Pt nanocomposite for improved antibacterial activity, *Colloids Surf., B* **103** (2013) 9-14.

[48] P. Boomi, H.G. Prabu, Synthesis, characterization and antibacterial analysis of polyaniline/Au–Pd nanocomposite, *Colloids Surf., A* **429** (2013) 51-59.

[49] A. Xie, F. Tao, L. Hu, Y. Li, W. Sun, C. Jiang, F. Cheng, S. Luo, C. Yao, Synthesis and enhanced electrochemical performance of Pt-Ag/porous polyaniline composites for glycerol oxidation, *Electrochim. Acta* **231** (2017) 502-510.

[50] A.P. Jonke, J.L. Steeb, M. Josowicz, J. Janata, Atomic clusters of Pd and $Au_NPd_M$ in polyaniline, *Catal. Lett.* **143** (2013) 531-538.

[51] M.E. Abdelhamid, G.A. Snook, A.P. O'Mullane, Electrochemical tailoring of fibrous polyaniline and electroless decoration with gold and platinum nanoparticles, *Langmuir* **32** (2016) 8834-8842.

[52] N.M. Ivanova, E.A. Soboleva, Y.A. Visurkhanova, Bimetallic Co–Cu polyaniline composites: Structure and electrocatalytic activity, *Russ. J. Appl. Chem.* **89** (2016) 1072-1081.

[53] T. Kessler, A.M. Castro Luna, A catalytic platinum–ruthenium–polyaniline electrode for methanol oxidation, *J. of Appl. Electrochem.* **32** (2002) 825-830.

[54] T, Kobayashi, H. Yoneyama, and H. Tamura, Polyaniline film-coated electrodes as electrochromic display devices, *J. Electroanal. Chem. Interfacial Electrochem.* **161** (1984) 419-423.

[55] R. Mazeikiene, A. Malinauskas, Kinetic study of the electrochemical degradation of polyaniline, *Synth. Met.* **123** (2001) 349-354.

[56] B. Wang, J. Tang, F. Wang, Electrochemical polymerization of aniline, *Synth. Met.* **18** (1987) 323-328.

[57] A.P. Jonke, J.L. Steeb, M. Josowicz, J. Janata, Atomic clusters of Pd and $Au_N Pd_M$ in polyaniline, *Catal. Lett.* **143** (2013) 531-538.

[58] E.M. Genies, C. Tsintavis, Electrochemical behaviour, chronocoulometric and kinetic study of the redox mechanism of polyaniline deposits, *J. Electroanal. Chem.* **200** (1986) 127-145.

[59] S. Trasatti, O.A. Petrii, Real surface area measurements in electrochemistry, *Pure Appl. Chem.* **63** (1991) 711-734.

[60] L. I. Elding, Palladium(II) halide complexes. I. Stabilities and spectra of palladium(II) chloro and bromo aqua complexes, *Inorg. Chim. Acta* **6** (1972) 647-651.

[61] J. A. Peck, C. D. Tait, B. I. Swanson, G. E. Brown Jr, Speciation of aqueous gold(III) chlorides from ultraviolet/visible absorption and Raman/resonance Raman spectroscopies, *Geochim. Cosmochim. Acta* **55** (1991) 671-676.

[62] D.W. Hatchett, N.M. Millick, J.M. Kinyanjui, S. Pookpanratana, M. Bär, T. Hofmann, A. Luinetti, C. Heske, The electrochemical reduction of PdCl4 2- and PdCl6 2- in polyaniline: Influence of Pd deposit morphology on methanol oxidation in alkaline solution, *Electrochim. Acta* **56** (2011) 6060-6070.

[63] H. T. Hien, H. T. Giang, N. V. Hieu, T. Trung, C. V. Tuan, Elaboration of Pd-nanoparticle decorated polyaniline films for room temperature NH3 gas sensors, *Sens. Actuators, B* **249** (2017) 348-356.

[64] J. B. Kortright and A. C. Thompson, *X-ray Data Booklet*. Lawrence Berkeley National Laboratory, University of California: Berkeley, CA, 2001.

[65] A.E. Bolzan, Phenomenological aspects related to the electrochemical behavior of smooth palladium electrodes in alkaline solutions, *J. Electroanal. Chem.* **380** (1995) 127-138.

[66] M. Grden, M. Lukaszewski, G. Jerkiewicz, A. Czerwinski, Electrochemical behavior of palladium electrode: oxidation, electrodissolution and ion adsorption, *Electrochim. Acta* **53** (2008) 7583-7598.

[67] K.A. Assiongbon, D. Roy, Electro-oxidation of methanol on gold in alkaline media: Adsorption characteristics of reaction intermediates studied using time resolved electro-chemical impedance and surface plasmon resonance techniques, *Surf. Sci.* **594** (2005) 99-119.

[68] S.J. Xia, V.I. Birss, In-Situ Quartz Crystal Microbalance Study of Au Oxide Growth in Alkaline Solution, *J. Electrochem. Soc. Proc.* **25** (2003) 171-180.

[69] M. Betowska-Brezezinska, T. Uczak, R. Holze, Electrocatalytic oxidation of mono- and polyhydric alcohols on gold and platinum, *J. Appl. Electrochem.* **27** (1997) 999-1011.

[70] J. Zhang, X. Ma, Z. Li, C. Dong, Electrocatalytic oxidation of four low-carbon alcohols at Pd nanoparticle modified indium tin oxide electrode, *J. Nanosci. Nanotechnol.* **14** (2014) 7242-7249.

[71] M. Simões, S. Baranton, C. Coutanceau, Electro-oxidation of glycerol at Pd based nano-catalysts for an application in alkaline fuel cells for chemicals and energy cogeneration, *Appl. Catal., B* **93** (2010) 354-362.

[72] J. Gong, D.W. Flaherty, T. Yan, C.B. Mullins, Selective oxidation of propanol on Au(111): mechanistic insights into aerobic oxidation of alcohols, *ChemPhysChem* **9** (2008) 2461-2466.

[73] J. Liu, J. Ye, C. Xu, S.P. Jiang, Y. Tong, Electro-oxidation of methanol, 1-propanol and 2-propanol on Pt and Pd in alkaline solution, *J. Power Sources* **177** (2008) 67-70.

[74] A. Nirmala Grace, K. Pandian, *Electrochem. Commun.* **8** (2006) 1340-1348.

[75] P. Boomi, H.G. Prabu, Synthesis, characterization and antibacterial analysis of polyaniline/Au–Pd nanocomposite, Colloids and Surfaces A: Physicochemical and Engineering Aspects, **429** (2013) 51-59.

[76] P. Boomi, H.G. Prabu, J. Mathiyarasu, Synthesis and characterization of polyaniline/Ag–Pt nanocomposite for improved antibacterial activity, *Colloids Surf., B* **103** (2013) 9-14.

[77] M.E. Abdelhamid, G.A. Snook, A.P. O'Mullane, Electrochemical tailoring of fibrous polyaniline and electroless decoration with gold and platinum nanoparticles, *Langmuir*, **32** (2016) 8834-8842.

[78] J. Tang, X.-C. Tian, W.-H. Pang, Y.-Q. Liu, J.-H. Lin, Codeposition of AuPd bimetallic nanoparticles on to ITO and their electrocatalytic properties for ethanol oxidation, *Electrochim. Acta* **81** (2012) 8-13.

[79] L. Qian, X. Yang, Dendrimer films as matrices for electrochemical fabrication of novel gold/palladium bimetallic nanostructures, *Talanta* **74** (2008) 1649-1653.

[80] S. Patra, S. Dash, V. Anand, C.S. Nimisha, G.M. Rao, N. Munichandraiah, Electrochemical co-deposition of bimetallic Pt–Ru nanoclusters dispersed on poly(3,4-ethylenedioxythiophene) and electrocatalytic behavior for methanol oxidation, *Mater. Sci. and Eng., B* **176** (2011) 785-791.

[81] M. Watanabe, S. Motoo, Electrocatalysis by ad-atoms: Part I. Enhancement of the oxidation of methanol on platinum and palladium by gold ad-atoms, *J. Electroanal. Chem. Interfacial Electrochem.* **60** (1975) 259-266.

[82] A. Dutta, A. Mondal, P. Broekmann, J. Datta, Optimal level of Au nanoparticles on Pd nanostructures providing remarkable electro-catalysis in direct ethanol fuel cells, *J. Power Sources* **361** (2017) 276-284.

[83] Y. Feng, Z. Liu, Y. Xu, P. Wang, W. Wang, D. Kong, Highly active PdAu alloy catalysts for ethanol electro-oxidation, *J. Power Sources* **232** (2013) 99-105.

[84] X. Wang, B. Tang, X. Huang, Y. Ma, Z. Zhang, High activity of novel nanoporous Pd–Au catalyst for methanol electro-oxidation in alkaline media, *J. Alloys Compd.* **565** (2013) 120-126.

[85] C. Hsu, C. Huang, Y. Hao, F. Liu, Au/Pd core-shell nanoparticles for enhanced electrocatalytic activity and durability, *Electrochem. Commun.* **23** (2012) 133-136.

[86] B. Hammer, J. K. Nørskov, Electronic factors determining the reactivity of metal surfaces, *Surf. Sci.* **343** (1995) 211-220.

[87] A.A. Rodriguez, C.T. Williams, J.R. Monnier, Effect of Structure and Substituents in the Aqueous Phase Oxidation of Alcohols and Polyols Over Au, Pd, and Au–Pd Catalysts, *Catal. Lett.* **145** (2015) 750-756.

88 T. Kessler, A.M. Castro Luna, A catalytic platinum–ruthenium–polyaniline electrode for methanol oxidation, J. Appl. Electrochem. **32** (2002) 825-830.

89 A. Xie, F. Tao, L. Hu, Y. Li, W. Sun, C. Jiang, F. Cheng, S. Luo, C. Yao, Synthesis and enhanced electrochemical performance of Pt-Ag/porous polyaniline composites for glycerol oxidation, Electrochim. Acta **231** (2017) 502-510.

[90] A.P. Jonke, J.L. Steeb, M. Josowicz, J. Janata, Atomic clusters of Pd and $Au_N Pd_M$ in polyaniline, *Catal. Lett.*, **143** (2013) 531-538.

[91] D.W. Hatchett, N.M. Millick, J.M. Kinyanjui, S. Pookpanratana, M. Bär, T. Hofmann, A. Luinetti, C. Heske, The electrochemical reduction of $PdCl_4^{2-}$ and $PdCl_6^{2-}$ in polyaniline: Influence of Pd deposit morphology on methanol oxidation in alkaline solution, *Electrochim. Acta* **56** (2011) 6060-6070.

[92] M. Muzikář, V. Komanický, W.R. Fawcett, A detailed study of gold single crystal growth in a silica gel, *J. Cryst. Growth* **290** (2006) 615-620.

[93] Y. Gao, A. Voigt, M. Zhou, K. Sundmacher, Synthesis of single-crystal gold nano- and microprisms using a solvent-reductant-template ionic liquid, *Eur. J. Inorg. Chem.* **2008** (2008) 3769-3775.

[94] D. A. J. Rand, R. Woods, Determination of the surface composition of smooth noble metal alloys by cyclic voltammetry, *J. Electroanal. Chem.* **36** (1972) 57-69.

[95] D. A. J. Rand, R. Woods, The electronic factor in catalysis by metals, *Surf. Sci.* **41** (1974) 611-614.

[96] M. Lukaszewski, A. Czerwinski, Electrochemical behavior of palladium-gold alloys, *Electrochim. Acta* **48** (2003) 2435-2445.

[97] R. Sharpe, J. Counsell, M. Bowker, Pd segregation to the surface of Au on Pd(111) and on Pd/TiO2(110), *Surf. Sci.* **656** (2017) 60-65.

Curriculum Vitae


Graduate College
University of Nevada, Las Vegas

Nicole Lyn Goodwin

Degrees:
      Bachelor of Science – Chemistry, 2010
      University of Nevada, Las Vegas

Publications:
      D. W. Hatchett, T. Quy, N. Goodwin, N. M. Millick, In-situ reduction of Au, Pd, and Pt metal precursors in polyaniline: Electrochemistry of variable metal content polymer/metal composites in alkaline solution, *Electrochim. Acta* **251** (2017) 699-709.

Dissertation Title: Controlled Electrochemical Reduction of Gold and Palladium Metal Precursors in Polyaniline

Dissertation Examination Committee:
      Chair, David Hatchett, Ph.D.
      Committee Member, Kathleen Robins, Ph.D
      Committee Member, Spencer Steinberg, Ph,D.
      Graduate Faculty Representative, Shawn Gerstenberger, Ph.D